

1 **How will the key marine calcifier *Emiliana huxleyi* respond to a warmer and**  
2 **more thermally variable ocean?**

3

4

5 Xinwei Wang<sup>1</sup>, Feixue Fu<sup>2</sup>, Pingping Qu<sup>2</sup>, Joshua D. Kling<sup>2</sup>, Haibo Jiang<sup>3</sup>, Yahui  
6 Gao<sup>1,4\*</sup>, David A. Hutchins<sup>2\*</sup>

7 *1. School of Life Sciences and State Key Laboratory of Marine Environmental Science,*  
8 *Xiamen University, Xiamen, 361102, China*

9 *2. Department of Biological Sciences, University of Southern California, Los Angeles,*  
10 *California, 90089, USA*

11 *3. School of Life Sciences, Central China Normal University, Wuhan, Hubei, China.*

12 *4. Key Laboratory of the Ministry of Education for Coastal and Wetland Ecosystems,*  
13 *Xiamen University, Xiamen 361102, China*

14

15 \*Corresponding authors: David Hutchins, tel: 1-213-7405616, fax: 1-213-7408123,

16 Email address: [dahutch@usc.edu](mailto:dahutch@usc.edu); Yahui Gao, tel/fax: 86-592-2181386, Email

17 address: [gaoyh@xmu.edu.cn](mailto:gaoyh@xmu.edu.cn)

18

19 Key words: thermal variation, *Emiliana huxleyi*, coccolithophore, calcification,  
20 growth rate, elemental composition, global warming

21 **Abstract**

22 Global warming will be combined with predicted increases in thermal variability in  
23 the future surface ocean, but how temperature dynamics will affect phytoplankton  
24 biology and biogeochemistry is largely unknown. Here, we examine the responses of  
25 the globally important marine coccolithophore *Emiliana huxleyi* to thermal variations  
26 at two frequencies (one-day and two-day) at low (18.5 °C) and high (25.5 °C) mean  
27 temperatures. Elevated temperature and thermal variation decreased growth,  
28 calcification and physiological rates, both individually and interactively. One-day  
29 thermal variation frequencies were less inhibitory than two-day variations under high  
30 temperature, indicating that high frequency thermal fluctuations may reduce heat-  
31 induced mortality and mitigate some impacts of extreme high temperature events.  
32 Cellular elemental composition and calcification was significantly affected by both  
33 thermal variation treatments relative to each other, and to the constant temperature  
34 controls. The negative effects of thermal variation on *E. huxleyi* growth rate and  
35 physiology are especially pronounced at high temperatures. These responses of the  
36 key marine calcifier *E. huxleyi* to warmer, more variable temperature regimes have  
37 potentially large implications for ocean productivity and marine biogeochemical  
38 cycles under a future changing climate.

39

## 40 **Introduction**

41 Climate-driven changes such as ocean warming alter the productivity and  
42 composition of marine phytoplankton communities, thereby influencing global  
43 biogeochemical cycles (Boyd et al., 2018; Hutchins & Fu, 2017; Thomas, et al., 2012).  
44 Increasing sea surface temperatures have been linked to global declines in  
45 phytoplankton concentration (Boyce et al., 2010), changes in spring bloom timing  
46 (Friedland et al., 2018), and biogeographic shifts in harmful algal blooms (Fu et al.  
47 2012; Gobler et al., 2017). Warming and acidification may drive shifts away from  
48 dinoflagellate or diatom dominance, and towards nanophytoplankton (Hare et al.,  
49 2007; Keys et al., 2018). Similarly, Morán et al. (2010) predicted that a gradual shift  
50 will occur towards smaller primary producers in a warmer ocean.

51 Effects of temperature increases on phytoplankton diversity are uncertain.  
52 Warming and phytoplankton biodiversity were found to be inversely correlated in a  
53 coastal California diatom assemblage, at least on short timescales (Tatters et al., 2018).  
54 In contrast, a five-year long mesocosm experiment found that elevated temperature  
55 can modulate species coexistence, thus increasing phytoplankton species richness and  
56 productivity (Yvon-Durocher et al. 2015). Globally, rising temperatures may result in  
57 losses of phytoplankton biodiversity in the tropics, but gains in the polar regions  
58 (Thomas et al., 2012). It is thought that ocean warming will lead to a poleward range  
59 expansion of warm-water species at the expense of cold-water species (Boyd et al.,  
60 2010; Gao et al., 2018; Hallegraeff, 2010; Hutchins & Fu, 2017; Thomas et al., 2012).  
61 It is evident that rising ocean temperatures will benefit some groups, while having

62 detrimental consequences for others (Boyd et al., 2010, 2015, 2018; Feng, et al., 2017;  
63 Fu et al., 2014). For example, recent decades of satellite observations show a striking  
64 poleward shift in the distribution of blooms of the coccolithophore *Emiliana huxleyi*,  
65 a species that was previously virtually absent in polar waters (Boyd et al., 2010;  
66 Neukermans et al., 2018).

67 Coccolithophores are the most successful calcifying phytoplankton in the ocean,  
68 and contribute almost half of global marine calcium carbonate production. They play  
69 crucial biogeochemical roles by performing both photosynthesis and calcification, and  
70 facilitate carbon export to the deep ocean through the ballasting effects of their  
71 calcium carbonate shells (Klaas & Archer, 2002; Krumhardt et al., 2017; Monteiro et  
72 al., 2016). *E. huxleyi* (Lohm.) is the most abundant and cosmopolitan coccolithophore,  
73 forming prolific blooms in many regions (Holligan, et al., 1983; 1993; Iglesias-  
74 Rodríguez et al., 2002; Westbroek et al., 1993).

75 The responses of *E. huxleyi* to global change factors have been intensively  
76 investigated. Many *E. huxleyi* strains are sensitive to ocean acidification, which  
77 negatively affects their growth rates and calcification (Feng et al., 2018; Hoppe et al.,  
78 2011). However, among the many currently changing environmental drivers,  
79 temperature may be among the most important in regulating coccolithophore  
80 physiology (Boyd et al., 2010). Feng et al. (2008) reported that the growth rate of *E.*  
81 *huxleyi* was improved by elevated temperature at low irradiance. Furthermore,  
82 temperature was the most important driver controlling both cellular particulate  
83 organic and inorganic carbon content of a Southern Hemisphere *E. huxleyi* strain

84 (Feng et al., 2018).

85 Most research about the effects of global warming on *E. huxleyi* and  
86 phytoplankton in general has focused on predicted increases in mean temperatures.  
87 However, in the natural environment, seawater temperatures fluctuate over timescales  
88 ranging from hours, to days, to months (Bozinovic et al., 2011; Jiang et al., 2017).  
89 Future climate models predict not only an increase in mean temperature, but also an  
90 increase in temperature variability (frequency and intensity), as well as a higher  
91 probability of extreme events (IPCC 2014).

92 The impacts of climatic variability and extremes have been best studied in  
93 metazoans, where they may sometimes have a larger effect than increases in climatic  
94 averages alone (Vázquez et al., 2017; Vasseur et al., 2014; Zander et al., 2017).  
95 Variability can promote greater zooplankton species richness, compared with  
96 long-term average conditions (Cáceres 1997; Shurin et al. 2010). In corals,  
97 temperature variability could buffer warming stress, elevate thermal tolerance and  
98 reduce the risk of bleaching (Oliver & Palumbi, 2011; Safaie et al., 2018).

99 In comparison, we still lack a thorough understanding of how thermal variation  
100 affects phytoplankton growth and physiology. Unlike zooplankton, the few available  
101 studies suggest increasing thermal variation may decrease phytoplankton biomass and  
102 biodiversity, and shift the community towards small phytoplankton (Burgmer &  
103 Hillebrand, 2011; Rasconi et al., 2017). Two studies have shown that plastic responses  
104 play a key role in acclimation and adaptation to thermal fluctuations in algae (Kremer  
105 et al., 2018; Schaum & Collins, 2014). Population growth rates of phytoplankton in

106 fluctuating thermal environments have been quantitatively modeled based on data  
107 from thermal response curves obtained under constant temperatures (Bernhardt et al.,  
108 2018).

109 In view of this relative lack of information on the effects of non-steady state  
110 temperatures on biogeochemically important phytoplankton, we carried out a thermal  
111 variability study using the Sargasso Sea *E. huxleyi* isolate CCMP371. Our  
112 experiments combined ocean warming with thermal variations, with a focus on the  
113 increasing frequency of temperature variations under global climate change. We  
114 examined growth rates, photosynthesis, calcification and elemental composition under  
115 constant, one-day and two-day temperature variations. This study is intended to  
116 provide insights into how different frequencies of thermal variation may influence the  
117 physiology and biogeochemistry of this important marine calcifying phytoplankton  
118 species under both current and future sea surface temperatures.

## 119 **Materials and methods**

120 The marine coccolithophore *E. huxleyi* (Lohm.) Hay and Mohler strain CCMP371  
121 (isolated from the Sargasso Sea) was maintained in the laboratory as stock batch  
122 cultures in Aquil medium ( $100 \mu\text{mol L}^{-1} \text{NO}_3^-$ ,  $10 \mu\text{mol L}^{-1} \text{PO}_4^{3-}$ ) made with  $0.2$   
123  $\mu\text{M}$ -filtered coastal seawater collected from the California region (Sunda et al., 2005).  
124 Cells were grown at  $22 \text{ }^\circ\text{C}$  under  $120 \mu\text{mol photons m}^{-2} \text{s}^{-1}$  cool white fluorescent  
125 light with a 12 h/12 h light/dark cycle.

## 126 **Experimental set-up**

127 An aluminum thermal gradient block with a range of 13 temperatures was used

128 to perform the thermal response curve and temperature variation experiments. For  
129 the thermal curve experiment, the extreme temperatures of the thermal-block were  
130 set to 8.5 °C and 28.6 °C, with intermediate temperatures of 10.5 °C, 12 °C, 13.5 °C,  
131 15.5 °C, 17.5 °C, 18.5 °C, 21.3 °C, 22.6 °C, 24.5 °C, 26.6 °C, and 27.6 °C. The *E.*  
132 *huxleyi* cells were transferred from the stock cultures into triplicate 120 ml acid  
133 washed polycarbonate bottles in the thermal block under a 12 h light /12h dark cycle  
134 at 180  $\mu\text{mol photons m}^{-2} \text{ s}^{-1}$ . For the light intensity measurement, irradiance was  
135 measured individually at each position in the thermal block using a light meter with a  
136 small detector bulb to fit into the round holes drilled to fit the experimental bottles  
137 (LI-250A light meter, LI-COR). During measurements the detector bulb was  
138 positioned identically in each position, and if necessary fluorescent lights were  
139 rearranged, added or removed until the light intensity was between 175-185  $\mu\text{mol}$   
140  $\text{photons m}^{-2} \text{ s}^{-1}$  for every experimental replicate.

141 Semi-continuous culturing methods were used for all experiments. Cultures were  
142 diluted with Aquil medium every two days to keep them in exponential growth stage  
143 while acclimating to the treatment temperatures for two weeks before starting the  
144 variation experiment. Dilution volumes were calculated to match growth rates of  
145 each individual replicate, as measured using *in vivo* chlorophyll a (Chl *a*)  
146 fluorescence. Once steady-state growth rates were recorded for 3–5 consecutive  
147 transfers, the cultures were sampled (Zhu et al., 2017). Due to the decrease of cell  
148 numbers during cultivation at 28.6 °C (from our preliminary experiment), these  
149 cultures were diluted from 22 °C stock cultures. They were then sampled as a batch

150 culture (without dilution) after 4-6 days to estimate the negative growth rates and  
151 elemental stoichiometry at this upper limit temperature point.

152 Six treatments were used to determine the responses of *E. huxleyi* growth,  
153 photosynthesis and calcification to different frequencies of temperature fluctuation.  
154 Temperature fluctuation treatments included: 1) Low temperature, constant (18.5  
155 °C). 2) Low temperature, one-day fluctuation cycle (16-21°C, mean = 18.5°C). 3)  
156 Low temperature, two-day fluctuation cycle (16-21°C, mean =18.5°C). 4) High  
157 temperature, constant (25.5 °C). 5) High temperature, one-day fluctuation cycle  
158 (23-28°C, mean = 25.5°C). 6) High temperature, two-day fluctuation cycle (23-28°C,  
159 mean = 25.5°C). For the variation treatment cycles, cultures were incubated at the  
160 cool phase (16 °C and 23 °C for low and high temperatures, respectively) for either  
161 one or two days. They were then transformed to the warm phase (21 °C and 28 °C for  
162 low and high temperature, respectively) for the same amount of time. It took about  
163 1/2 hour to re-adjust the thermal block to the transformed temperature at the  
164 beginning of each new treatment cycle. The experimental *E. huxleyi* cultures were  
165 grown in triplicate in 120 ml acid washed polycarbonate bottles using the  
166 thermal-block under a 12 h light /12h dark cycle at 180  $\mu\text{mol photons m}^{-2} \text{ s}^{-1}$ .

167 For the variable temperature experiment, cultures were diluted semi-continuously  
168 with Aquil medium every two days the for constant and one-day variation treatments,  
169 and every four days for two-day variation treatments. To ensure nutrient-replete  
170 conditions in the two-day variation treatments, Aquil nitrate and phosphate stocks  
171 were added at the two day midpoint of every four day thermal cycle to make sure

172 that the final nitrate and phosphate concentrations were not depleted and were  
173 always maintained  $>100 \mu\text{mol L}^{-1}$  and  $>10 \mu\text{mol L}^{-1}$ , respectively. Cultures were  
174 grown for at least eight dilutions (~16 days for constant and one day variation  
175 treatments; ~32 days for two-day variation treatments) to acclimate to the different  
176 experimental conditions before final sampling. All variation treatments were  
177 sampled twice across the thermal variation cycle, once during the cool phase and  
178 once during the warm phase.

### 179 **Growth rates**

180 *In vivo* fluorescence was measured daily for the one-day variation treatment and  
181 every two days for the constant and two-day variation treatments using a Turner  
182 10-AU fluorometer (Turner Designs, CA). *In vivo*-derived growth rates were  
183 subsequently verified using cell samples counted with a nanoplankton counting  
184 chamber on an Olympus BX51 microscope. Specific growth rates ( $\text{d}^{-1}$ ) were  
185 calculated using the *in vivo* fluorescence and cell count data as:  
186  $\mu = \ln[N(T_2)/N(T_1)]/(T_2 - T_1)$ , in which  $N(T_1)$  and  $N(T_2)$  are the *in vivo* fluorescence  
187 values (for thermal curve experiments and constant treatments) or cell counts (for  
188 variation treatments, because of potential changes in cellular *in vivo* fluorescence  
189 during fluctuation) at  $T_1$  and  $T_2$ .

### 190 **Chl *a* analysis**

191 Twenty ml culture samples were filtered onto GF/F glass fiber filters (Whatman,  
192 Maidstone, UK) for Chl *a* analysis. In vitro Chl *a* was extracted with 90% aqueous  
193 acetone for 24 hours at  $-20 \text{ }^\circ\text{C}$ , and then measured using a Turner 10-AU fluorometer

194 (Turner Design, USA). (Fu et al., 2007).

### 195 **Elemental analysis**

196 Elemental composition sampling included total particulate carbon (TPC),  
197 particulate organic carbon (POC), particulate organic nitrogen (PON), particulate  
198 inorganic carbon (PIC) and particulate organic phosphorus (POP), allowing  
199 calculation of cellular elemental stoichiometry and calcite/organic carbon ratios  
200 (PIC/POC) (Feng et al.; 2008). Culture samples for TPC, POC and PON, were  
201 collected onto pre-combusted GF/F glass fiber filters (Whatman) and dried in a 60  
202 °C oven overnight. For POC analysis, filters were fumed for 24 hours with  
203 saturated HCl (~37%) to remove all inorganic carbon prior to analysis. TPC, PON  
204 and POC were then measured by a 440 Elemental Analyzer (Costech Inc, CA)  
205 according to the previous studies (Hutchins et al., 1998; Feng et al., 2008). PIC was  
206 calculated as the difference between TPC and POC. For POP measurement, culture  
207 samples were filtered on onto pre-combusted GF/F filters (Whatman) and analyzed  
208 using a molybdate colorimetric method (Solórzano and Sharp, 1980), with minor  
209 modifications as in Fu et al. (2007).

### 210 **Total carbon fixation, photosynthetic and calcification rates & ratios**

211 Total carbon fixation, photosynthetic carbon fixation and calcification rates were  
212 measured using a <sup>14</sup>C incubation techniques (Platt et al., 1980) with slight  
213 modifications as in Feng et al. (2008). Sixty mL culture samples from each treatment  
214 were spiked with 0.2 µCi NaH<sup>14</sup>CO<sub>3</sub> and then incubated for 4 h under their  
215 respective experimental conditions. After incubation, samples were filtered on two

216 Whatman GF/F filters (30mL each) for total carbon fixation and photosynthetic rate  
217 separately. The filters for photosynthetic rate measurement were fumed with  
218 saturated HCl (~37%) before adding scintillation fluid. Thirty mL from each  
219 treatment (10 mL from each replicate bottle) was filtered immediately, after adding  
220 equal amounts of  $\text{NaH}^{14}\text{CO}_3$  for procedural filter blanks. Filters were then placed in  
221 7 mL scintillation vials with 4 mL scintillation fluid overnight in the dark. To  
222 determine the total radioactivity (TA), 0.2  $\mu\text{Ci}$   $\text{NaH}^{14}\text{CO}_3$  together with 100  $\mu\text{L}$   
223 phenylalanine was placed in scintillation vials with the addition of 4 mL scintillation  
224 solution. All samples were counted on a Perkin Elmer Liquid Scintillation Counter to  
225 measure the radioactivity. Total carbon fixation and photosynthetic rate were  
226 calculated from TA, final radioactivity and total dissolved inorganic carbon (DIC)  
227 values. Calcification rate was then calculated as the difference between total carbon  
228 fixation and photosynthetic rate for each sample.

### 229 **Model for population growth of *E. huxleyi***

230 Growth rates measured under constant temperatures in the thermal block were  
231 fitted to the Eppley thermal performance curve (Eppley, 1972; Norberg, 2004;  
232 Thomas et al., 2012). This function quantifies parameters of growth temperature  
233 effects, including the temperature optimum for growth ( $T_{\text{opt}}$ ), and high and low  
234 temperature limits ( $T_{\text{max}}$  and  $T_{\text{min}}$  respectively) in our strain of *E. huxleyi*. A model  
235 based on the Eppley curve but incorporating non-linear averaging and consideration  
236 of Jensen's inequality (Bernhardt et al., 2018) was applied to predict the impact that  
237 fluctuating temperatures might have on the shape of thermal growth curves at

238 present-day and future mean temperatures, similar to other recent studies (Qu et al.  
239 2019, Kling et al. in press).

#### 240 **Statistical analysis**

241 The mean values of most parameters measured under the variation treatments  
242 were calculated by averaging the values from the cool and warm phases, including  
243 all the elemental content and ratios, photosynthetic and calcification rates and ratios.  
244 For the statistical analyses, the Student's t-test and one-way ANOVA were applied  
245 to analyze the difference among temperature treatments. *p*-values were calculated  
246 based on two formulas including `compare_means()` and `stat_compare_mean()` via the  
247 `ggpubr` package, and the figures were generated via the `ggplot` package in open  
248 source statistical software R version 3.5.0 (R Foundation).

#### 249 **Results**

##### 250 **Responses of *E. huxleyi* to warming**

251 The growth rates of *E. huxleyi* at constant temperature increased significantly  
252 with warming from  $0.09 \pm 0.01 \text{ d}^{-1}$  at 8.5 °C to a maximum value of  $0.90 \pm 0.02 \text{ d}^{-1}$  at  
253 21.3 °C. Growth was optimal up to 24.5 °C, and then decreased rapidly to  $-0.46 \pm 0.05$   
254  $\text{d}^{-1}$  at 28.6 °C ( $p < 0.05$ , Fig. 1).

255 The elemental ratios of the cells in the different temperature treatments were  
256 compared to the average elemental ratios across the entire temperature range (Fig. 2).

257 The thermal trends of TPC/PON ratios were generally similar with those of growth  
258 rates, in that ratios increased from 8.5 to 17.5 °C, and then decreased from 24.5 to  
259 27.6 °C. The TPC/PON ratios at 8.5, 10.5 and 27.6 °C were significantly lower than

260 the average level of all the temperature points ( $p < 0.05$ , Fig 2A). The POC/PON  
261 ratios of most temperature points were very close to the mean value of 6.3, except at  
262 27.6 °C (7.1) and 28.6 °C (7.4), which were significantly higher than the average  
263 ( $p < 0.05$ , Fig 2B). The highest PIC/POC ratio was  $0.49 \pm 0.07$  at 22.6 °C, and the  
264 lowest PIC/POC ratio was  $0.05 \pm 0.04$  at 27.6 °C, a value that was almost 90% less  
265 than the highest value. The PIC/POC ratios at the lowest temperature tested (10.5 °C)  
266 and at the high end of the temperature range (26.6 and 27.6 °C) were significantly  
267 lower than the average level (Fig. 2C). Chl *a*/POC ratios were significant lower at  
268 8.5, 10.5 and 27.6 °C than the mean, and at 17.5, 21.3, 22.6 and 24.5 °C were  
269 significantly higher than the average ( $p < 0.05$ , Fig. 2C). The trends of PIC/POC and  
270 Chl *a*/POC ratio were similar, in that they gradually increased from low temperature  
271 and to the highest value at 22.6 °C, and then dropped rapidly as temperature  
272 increased further. (Fig. 2C, D).

### 273 **Responses of *E. huxleyi* to temperature variations**

#### 274 **Growth rate**

275 In low temperature experiments, both one-day and two-day temperature  
276 variations had a negative effect on growth rate. The mean growth rates of the  
277 one-day ( $0.71 \pm 0.01 \text{ d}^{-1}$ ) and two-day ( $0.72 \pm 0.01 \text{ d}^{-1}$ ) variation treatments were not  
278 significantly different from each other ( $p > 0.05$ ), but both were lower than that of the  
279 constant 18.5 °C treatment ( $0.76 \pm 0.01$ ,  $p < 0.05$ ) (Fig. 3A). Growth rates were low  
280 during the cool phase (16 °C) of the experiment ( $\sim 0.5\text{-}0.6 \text{ d}^{-1}$ ), but those of the  
281 two-day variation cycle were not significantly different from the constant control at

282 this temperature ( $p > 0.05$ ). However, the growth rates during the cool phase of the  
283 one-day variation cycle were lower than those of the constant 16 °C treatment  
284 ( $p < 0.05$ ). During the warm phase of the thermal cycle (21°C), there were no  
285 significant differences in the elevated growth rates ( $\sim 0.85\text{--}0.9\text{ d}^{-1}$ ) of the constant  
286 control and those of either variable treatment ( $p > 0.05$ , Fig. 3A).

287 In the high temperature experiments, as in the low temperature experiments, both  
288 temperature variation frequencies had a negative effect on mean growth rates. The  
289 growth rates in the two-day variation treatment were ( $0.20 \pm 0.02\text{ d}^{-1}$ ), a decrease of  
290  $\sim 74\%$  compared with the constant 25.5 °C ( $p < 0.05$ ), and  $\sim 62\%$  of the one-day  
291 variation treatment value ( $p < 0.05$ , Fig. 3B). During the cool phase (23 °C), the  
292 growth rate of the one-day variation treatment was slightly lower ( $p < 0.05$ ) than the  
293 constant 23 °C, but there were no significant changes between two-day variations  
294 and the constant 23 °C treatment ( $p > 0.05$ , Fig. 3B). During the warm phase (28 °C),  
295 the constant 28 °C and two-day variation treatment both had negative growth rates of  
296  $-0.45 \pm 0.05\text{ d}^{-1}$  and  $-0.45 \pm 0.04\text{ d}^{-1}$ , respectively. However, the one-day variation  
297 treatment had a low but positive warm phase growth rate at  $0.25 \pm 0.02\text{ d}^{-1}$  (Fig. 3B).  
298 There was a time lag of  $\sim 1/2$  hour to switch to the transformed temperature for each  
299 new growth phase, which should thus have had only minimal effects on overall  
300 growth rates across the one-day and two-day thermal variations.

### 301 Cellular PIC and POC contents and ratios

302 In low temperature experiments, the cellular PIC content of the constant 18.5 °C  
303 treatment was  $3.5 \pm 0.3\text{ pg/cell}$ , and there were no significant differences with

304 temperature variation treatments ( $p > 0.05$ , Table 1). However, the cellular POC  
305 content of the constant 18.5 °C treatment was  $8.0 \pm 0.6$  pg/cell, which was lower than  
306 in the two-day variation treatment, but significantly higher than in the one-day  
307 variation treatment ( $p < 0.05$ ).

308 Like POC, the PIC/POC ratio was significantly affected by temperature  
309 variations (Fig. 4A). The lowest PIC/POC ratio was found in the one-day variation  
310 treatment ( $0.38 \pm 0.07$ ), which was significantly lower than the two-day variation  
311 treatment value ( $p < 0.05$ ), but close to that in the constant 18.5 °C ( $p > 0.05$ ). A  
312 similar trend was found in both the cool (16 °C) and warm phases (21 °C) of the two  
313 variation treatments, in that the PIC/POC ratio of the one-day variation treatment  
314 was lower than of the two-day variation treatment ( $p < 0.05$ , Fig. 4A). Both variation  
315 treatments had lower PIC/POC ratios during the warm phase than during the cool  
316 phase, although these differences were not significant ( $p > 0.05$ ).

317 High temperature experiments showed particulate carbon trends that were  
318 contrary to those of the low temperature treatments. The PIC content and PIC/POC  
319 ratios were significantly decreased by temperature variation. The cellular PIC  
320 content of the constant treatment (25.5 °C) was  $5.5 \pm 0.3$  pg/cell, which was ~ 200%  
321 higher than that of the one-day variation and ~ 160% higher than in the two-day  
322 variation treatments ( $p < 0.05$ , Table 1). The same trend was found for PIC/POC  
323 ratios in one-day variation and two-day variation treatments, which decreased ~ 67%  
324 and 33% compared with the constant 25.5 °C treatment, respectively ( $p < 0.05$ , Fig.  
325 4B). However, the POC content of one-day and two-day variation treatments was

326 higher than in the constant 25.5 °C treatment ( $p < 0.05$ , Table 1). During the cool  
327 phase (23 °C), the PIC content and PIC/POC ratio of the one-day variation treatment  
328 was significantly lower than in the two-day variation treatment, but contrary to PIC  
329 content, the POC content of the one-day variation treatment was significantly higher  
330 than that in the two-day variation treatment. During the warm phase (28 °C), there  
331 were no significant differences of PIC content, POC content, or PIC/POC ratio  
332 between the one-day and two-day variation treatments (Fig. 4B, Table 1).

### 333 **Photosynthetic and calcification rates and ratios**

334 In low temperature treatments, there were no differences between total carbon  
335 fixation rates (photosynthesis plus calcification) for the two variable treatments  
336 relative to the constant control (Fig. 5A). However, during the cool phase total  
337 carbon fixation rates were higher in the one-day variation than in the two-day  
338 variation ( $p < 0.05$ , Fig 5A), while this rate was the same in both variation treatments  
339 during the warm phase ( $p > 0.05$ , Fig. 5A). In high temperature experiments, the  
340 total carbon fixation rates of the one-day and two-day variation treatments were  
341 significantly decreased by about ~20% and ~18% respectively, compared with the  
342 constant 25.5 °C treatment ( $p < 0.05$ , Fig. 5 B).

343 The photosynthetic and calcification rates of the constant 18.5 °C treatment were  
344  $0.04 \pm 0.00$  pmol C cell<sup>-1</sup> hr<sup>-1</sup> and  $0.02 \pm 0.00$  pmol C cell<sup>-1</sup> hr<sup>-1</sup>, respectively, which  
345 were not significantly different from both of the temperature variation treatments ( $p >$   
346  $0.05$ , Fig. 5 C,E). Photosynthetic rates changed within the thermal cycle for both  
347 one-day and two-day variation treatments, with a decrease of 22% and 28% from the

348 warm phase to the cool phase, respectively (Fig. 5C). However, there were no  
349 significant changes in calcification rates under either variation frequency treatment  
350 between the cool and warm phases of the thermal cycles ( $p > 0.05$ ).

351 In the mean 25.5 °C experiment, photosynthetic rates were not significantly  
352 different between the one-day variation and constant treatments ( $p > 0.05$ ), while the  
353 photosynthetic rate of the two-day variation was slightly higher than that of the  
354 constant 25.5 °C treatment ( $p < 0.05$ , Fig. 5D). In contrast, calcification rates of  
355 one-day and two-day variation treatments at a mean temperature of 25.5 ° were  
356 significantly decreased by about ~46% and ~51%, respectively, relative to the  
357 constant control ( $p < 0.05$ , Fig. 5F). There were no significant differences in total  
358 carbon fixation, photosynthetic and calcification rates between the one-day variation  
359 and two-day variation treatments during both the cool (23 °C) and warm (28 °C)  
360 phases ( $p > 0.05$ , Fig. 5 B,D,F).

361 In the low temperature treatments, there were no significant differences in  
362 Cal/Photo ratios between the constant and the two variable treatments ( $p > 0.05$ , Fig  
363 6A). In contrast, in the high temperature experiments, the Cal/Photo ratio of the  
364 one-day variation and two-day variation treatments were decreased by ~40% and  
365 49%, respectively, compared with the constant 25.5 °C treatment ( $p < 0.05$ , Fig. 6B).  
366 For both low and high temperature experiments, there were no significant differences  
367 between the one-day and two-day variation treatments in either the cool or warm  
368 phases of the thermal cycle ( $p > 0.05$ , Fig. 6B). However, in both temperature  
369 treatments the lower photosynthetic rates during the cool phase (Fig. 5C,D) resulted

370 in an increase in the Cal/Photo ratio during the cool phase for both the one-day and  
371 two-day variation treatments ( $p < 0.05$  Fig. 6A,B).

372

### 373 **Elemental content and stoichiometry**

374 In the low temperature experiments, the one-day variation and two-day thermal  
375 variations had different effects on cellular elemental contents and ratios, relative to  
376 the constant 18.5 °C treatment. One-day variation increased most of the cellular  
377 elemental and biochemical contents (TPC, PON, and Chl *a*) but with no significant  
378 difference ( $p > 0.05$ ), except for POP content ( $p < 0.05$ ), compared with the constant  
379 18.5 °C treatment (Table 1). In contrast, the two-day variation treatment decreased  
380 all the measured cellular elemental and biochemical contents (TPC, PON, POP and  
381 Chl *a*,  $p < 0.05$ ) in relation to the constant 18.5 °C treatment (Table 1). However, the  
382 TPC/PON and Chl *a*/POC ratios of the two-day variation treatment were higher than  
383 those of the one-day variation and constant 18.5 °C treatments ( $p < 0.05$ , Fig. 7A,E),  
384 while the PON/POP ratio was lower than in the one-day variation and constant 18.5  
385 °C treatments ( $p < 0.05$ , Fig. 7C). There were no significant differences in TPC/PON,  
386 PON/POP and Chl *a*/POC ratios between the constant 18.5 °C and the one-day  
387 variation treatments ( $p > 0.05$ , Fig. 7A).

388 In high temperature experiments, the highest cellular TPC, PON and POP  
389 contents were all obtained under the one-day variation treatment, which was  
390 significantly higher than under constant 25.5 °C conditions ( $p < 0.05$ , Table 1).  
391 However, there were no significant differences in cellular Chl *a* content between the

392 constant 25.5 °C and both variation treatments ( $p > 0.05$ , Table 1). The TPC/PON  
393 ratio of the constant 25.5 °C treatment was ~22% and ~35% higher than that of the  
394 two-day variation and one-day variation treatments, respectively ( $p < 0.05$ , Fig. 7B),  
395 while the PON/POP ratio was highest in the **one-day** variation, followed by the  
396 two-day variation and finally by the constant control (Fig. 7D). The Chl *a*/POC ratio  
397 of the one-day variation treatment was significantly lower than that of the constant  
398 25.5 °C and two-day variation treatments ( $p < 0.05$ ), but there were no significant  
399 differences between the constant 25.5 °C and two-day variation treatments ( $p > 0.05$ ,  
400 Fig. 7F).

401 During the cool phase of the high temperature experiments (23 °C), the cellular  
402 TPC, PON, POP and Chl *a* content of two-day variation were all significantly lower  
403 than in the one-day variation treatment ( $p < 0.05$ ). Similar decreasing trends during  
404 the cool phase were observed for the TPC/PON ratios (Fig. 7B), but not the Chl  
405 *a*/POC ratio, which was ~32% higher than in the one-day variation treatment ( $p < 0.05$ ,  
406 Fig. 7F). During the warm phase (28 °C), there were no significant differences of  
407 cellular TPC, PON and POP contents between one-day and two-day variation  
408 treatments ( $p > 0.05$ , Table 1) as well as the TPC/PON ratio (Fig 7B). However, the  
409 Chl *a* content of the one-day variation treatment was ~20% lower than that of the  
410 two-day variation treatment ( $p < 0.05$ ). The Chl *a*/POC ratio was not significantly  
411 different between the one-day and two-day variation treatments at the warm phase  
412 ( $p > 0.05$ , Table 1, Fig. 7F).

413 **Experimental constant temperature performance curves and measured and**

414 **modeled fluctuating temperature performance curves**

415 The experimentally-determined constant condition temperature performance  
416 curves and the predicted fluctuating temperature condition temperature performance  
417 curves based on the Bernhardt et al. (2018) non-linear averaging model are shown in  
418 Fig. 8 for *E. huxleyi*. Compared with the measured temperature performance curve  
419 under constant thermal conditions, the modeled curve of the fluctuating temperature  
420 condition showed a leftward shift towards lower temperatures at optimum  
421 temperatures and above. The maximum and optimal temperature of the modeled  
422 fluctuating temperature performance curve were all lower than those of the measured  
423 constant condition curve. In particular, the optimal temperature for growth decreased  
424 from 22°C in constant conditions to 21 °C under fluctuating temperature conditions.  
425 At the same time, the maximum growth rate ( $\mu_{\max}$ ) of the fluctuating temperature  
426 condition was 0.8 d<sup>-1</sup>, which was lower than the constant condition value of 0.9 d<sup>-1</sup>.  
427 The measured growth rates of experimental one-day (0.71 d<sup>-1</sup>) and two-day (0.72 d<sup>-1</sup>)  
428 variation treatments at the relatively low mean temperature of 18.5 °C closely  
429 matched the model-predicted fluctuating temperature growth rate at this temperature  
430 (0.74<sup>-1</sup>, Fig. 8). However, measured and predicted growth rates did not match as well  
431 at the higher mean temperature. At 25.5 °C, the measured growth rate of the one-day  
432 variation was 0.52 d<sup>-1</sup>, 30% higher than the predicted fluctuating temperature growth  
433 rate of 0.40 d<sup>-1</sup>. In contrast, the measured growth rate of the experimental two-day  
434 variation treatment was 0.20 d<sup>-1</sup>, a decrease of 50% compared to the model-predicted  
435 fluctuating temperature growth rate of 0.40 d<sup>-1</sup> at this temperature (Fig. 8).

436 **Discussion**

437 **Effects of warming on *Emiliana huxleyi* growth rates and elemental ratios**

438 Thermal response curves and optimum growth temperatures describe the  
439 importance of temperature as a control on the distribution of *E. huxleyi* strains in the  
440 ocean (Buitenhuis et al., 2008; Paasche, 2001). The optimal temperature range of  
441 21.3-24.5 °C found in our study is similar to that of some other *E. huxleyi* strains (De  
442 Bodt et al., 2010; Feng et al., 2017; Rosas-Navarro et al., 2016; Zhang et al., 2014).  
443 Most studies have focused on the lower part of the temperature curve where growth  
444 rates increase with rising temperatures (Feng et al., 2017; Matson et al., 2016), with  
445 relatively few examining stressfully warm temperatures where growth is inhibited  
446 (Zhang et al., 2014). In our study, the descending portion of the upper temperature  
447 performance curve ranged from 24.5 °C to 28.6 °C, at which point growth rates  
448 became negative. This *E. huxleyi* strain was isolated from the Sargasso Sea where the  
449 sea surface temperature can reach 29 °C in the summer, and will be higher in the  
450 future with global warming  
451 (<https://seatemperature.info/sargasso-sea-water-temperature.html>). This suggests that  
452 this strain may be currently living near its upper thermal limit for part of the year, as  
453 are many other tropical and subtropical phytoplankton (Thomas et al. 2012), and that  
454 it may therefore be vulnerable to further warming.

455 Calcification is the key biogeochemical functional trait of this species, and the  
456 PIC/POC ratio of *E. huxleyi* can be influenced by factors that include CO<sub>2</sub>  
457 concentration, nutrient status, irradiance and temperature (Feng et al., 2008, 2017;

458 Raven & Crawford, 2012). The cellular PIC/POC of *E. huxleyi* has been reported to  
459 decrease as irradiance and CO<sub>2</sub> concentration rises, but increase under nitrate and  
460 phosphate limitation (Feng et al., 2017; Paasche, 1999; Riegman et al., 2000). The  
461 effect of temperature on *E. huxleyi* cellular PIC/POC ratio is however more complex.  
462 De Bodt et al. (2010) and Gerech et al. (2014) observed that higher cellular PIC/POC  
463 ratios were obtained at lower temperatures for both *E. huxleyi* and *Coccolithus*  
464 *pelagicus*. Sett et al. (2014), however, found an opposite trend, whereby the PIC/POC  
465 ratio increased with temperature in another strain of *E. huxleyi*. Feng et al. (2017)  
466 reported that the cellular PIC/POC of *E. huxleyi* was increased as the temperature rose  
467 from 4 °C to 11 °C, but decreased with warming from 11 °C to 15 °C and remained  
468 steady afterwards.

469 In our study, the cellular PIC/POC ratio of *E. huxleyi* was positively correlated to  
470 growth rate ( $R^2=0.73$ ), and increased with warming from 8.5 °C to a maximum at 22.6  
471 °C, and then decreased with further warming to 27.6 °C. In a meta-analysis of studies  
472 using different coccolithophore subgroups, Krumhardt et al. (2017) found that the  
473 highest PIC/POC ratios were observed between 15 °C and 20 °C, in the same thermal  
474 range where the highest growth rates of *E. huxleyi* are found, as seen here and in Sett  
475 et al. (2014). In contrast, Rosas-Navarro et al. (2016) reported that the cellular  
476 PIC/POC ratio showed a minimum at optimal growth temperature (between 20 and  
477 25 °C) for three strains of *E. huxleyi*. However, the *E. huxleyi* strain used here was  
478 isolated from a warmer area (the Sargasso Sea) compared with isolates from coastal  
479 Japan and New Zealand in previous studies (Rosas-Navarro et al. 2016; Feng et al.

480 2017). The growth temperature for our stock cultures was 22-24°C, higher than that of  
481 the other two *E. huxleyi* strains. Feng et al. (2017) also found that the optimal  
482 temperature for calcification was close to the stock culture maintenance temperature  
483 in their study. Our results also support suggestions that stressful high temperatures  
484 may lead to decreases in cellular PIC/POC ratios and calcification (De Bodt et al.,  
485 2010; Feng et al., 2017; Gerecht et al., 2014; Krumhardt et al., 2017). **The cellular  
486 PIC/POC ratio of *E. huxleyi* was much more plastic than the other ratios we measured,  
487 including TPC/PON and POC/PON. Indeed, PIC/POC ratios may change  
488 dramatically (>2-fold) with temperature for some coccolithophore subgroups  
489 (Krumhardt et al., 2017). The plasticity in PIC/POC ratios of *E. huxleyi* during  
490 temperature changes in our study may have implications for shifts in the ballasting of  
491 coccolith-containing particles during sinking, thus affecting the ocean carbon cycle.**

492 The cellular Chl *a*/POC ratio of *E. huxleyi* showed a similar pattern with the  
493 PIC/POC ratio, as it was also positively correlated to growth rate. Zhu et al. (2017)  
494 reported the cellular Chl *a*/POC ratio of a Southern California diatom was also  
495 correlated to growth rate across a very similar temperature range. In contrast, Feng et  
496 al. (2017) found that the cellular Chl *a*/POC ratio of *E. huxleyi* dramatically decreased  
497 with warming. However, in our experiments, the cellular Chl *a*/POC ratio was lower  
498 at 27.6 °C than at 28.6 °C, likely due to the negative growth rates and consequent lack  
499 of acclimation of the cultures maintained at the highest temperature. Traits such as  
500 PIC/POC ratios, Chl *a*/POC ratios and TPC/PON ratios also showed some evidence  
501 for possible carryover from the stock cultures (22-24 °C) in this 28.6 °C treatment, as

502 we were forced to sample before the cells died completely, after only 2-3 cycles of  
503 dilution.

## 504 **Effect of thermal variation on *Emiliania huxleyi* growth and physiology**

### 505 *Constant vs variable temperature*

506 Thermal variability in the surface ocean is becoming an increasingly relevant  
507 topic as global warming proceeds. In our study, we found that the growth rates of a  
508 subtropical *E. huxleyi* strain were quite sensitive to temperature variation under both  
509 low (18.5 °C, “winter”) and high (25.5 °C, “summer”) mean temperatures. In both  
510 low and high temperature experiments, growth rates always decreased under  
511 temperature variation, compared with the constant mean temperature. This result  
512 agrees with previous studies showing that temperature variation slowed the growth  
513 rates of the fresh water green alga *Chlorella pyrenoidosa* and the marine diatom  
514 *Cyclotella meneghiniana*, as observed in laboratory work but also during long-term  
515 field observations (Zhang et al., 2016).

516 This growth rate inhibition under temperature variation was more pronounced at  
517 high temperature than at low temperature, indicating that variability at the warm  
518 range boundary will have a stronger negative effect on population growth rate than  
519 variability near the lower thermal limits (Bernhardt et al., 2018). **This trend suggests**  
520 **that acclimation to high temperature (whether constant or variable) may require**  
521 **greater investment in cellular repair machinery, such as heat shock proteins, thus**  
522 **potentially diverting nutrient and energy supplies and thereby reducing growth rates**  
523 **(O'Donnell et al., 2018).** However, following Jensen’s inequality model to predict

524 the thermal performance curve, there should be an inflection point where the transfer  
525 between positive and negative effects of temperature variability will occur compared  
526 with the constant thermal curve. Conversely, for phytoplankton living in regions of  
527 suboptimal temperatures, thermal variation can enhance growth (Bernhardt et al.,  
528 2018). Thus, for some polar phytoplankton or for temperate species extending their  
529 ranges poleward, such as *E. huxleyi* (Neukermans et al., 2018), not only warming but  
530 also thermal variability may need to be taken into consideration in order to  
531 understand changes in high latitude microbial communities and biogeochemistry  
532 cycles.

533 Temperature variation affected the physiology of *E. huxleyi* differently  
534 compared with constant temperature. Physiological traits that were affected by  
535 thermal fluctuations also differed at low temperature (“winter”) and high temperature  
536 (“summer”), suggesting different response mechanisms. Under low temperature  
537 variations (16-21 °C), photosynthesis and calcification were correlated with  
538 temperature, leading to rates similar to those observed with constant temperature.  
539 However, elemental contents and ratios under thermal variations differed from  
540 constant temperature. For instance, the cellular POC, PON, POP and Chl *a* contents  
541 increased during one-day variations but decreased during two-day variations,  
542 compared with constant temperature.

543 These cellular quota changes were reflected in elemental ratio differences  
544 (PIC/POC, Chl *a*/POC and TPC/POC) between the thermal variation treatments and  
545 constant temperature. However, the changes between thermal variation and constant

546 treatments were not significant under low temperature (“winter”), indicating that the  
547 thermal variation wouldn’t significantly influence biogeochemical cycles under these  
548 conditions. Unlike constant temperature treatments where selection may favor a  
549 higher growth rate, the trade-off for the thermal variation treatments may involve  
550 sacrificing increased growth rate in order to adjust cellular stoichiometry to adapt to  
551 the fluctuating environment.

552 In contrast, photosynthetic and calcification rates under high temperature  
553 thermal variations (23-28 °C) were significantly different from those seen under  
554 constant temperature (25 °C), especially the calcification rate. Thermal variation  
555 treatments transiently but repeatedly experienced the extreme high temperature point  
556 (28 °C), leading to extremely low calcification rates and PIC contents, and thus  
557 relatively low PIC/POC and Cal/Photo ratios. Previous *E. huxleyi* studies agree that  
558 high temperature decreases PIC content, PIC/POC ratios and Cal/Photo ratios (Feng  
559 et al., 2017; 2018; Gerecht et al., 2014). The two different patterns of responses to  
560 thermal variation we observed under low and high temperatures imply a seasonal  
561 pattern in the ways that thermal variations will affect the elemental stoichiometry of  
562 *E. huxleyi*.

563 Under other stresses such as nutrient limitation, trade-offs between growth rates  
564 and resource affinities may be necessary to adapt to thermal changes. For instance,  
565 nitrate affinity declines in cultures of the large centric diatom *Coscinodiscus*  
566 acclimated to warmer temperatures (Qu et al. 2018), while warming decreases  
567 cellular requirements for iron in the nitrogen-fixing cyanobacterium *Trichodesmium*

568 (Jiang et al. 2018). In nitrogen-limited cultures of the marine diatom *Thalassiosira*  
569 *pseudonana*, long-term thermal adaptation acted most strongly on systems other than  
570 those involved in nitrate uptake and utilization (O'Donnell et al., 2018). Thus, it is  
571 possible that our thermal response results with *E. huxleyi* might have differed under  
572 nutrient-limited growth conditions.

### 573 ***One-day vs two-day thermal variation***

574 As temperature fluctuations in the surface ocean increase along with climate  
575 change, phytoplankton will be influenced by the frequencies and intensities of these  
576 thermal excursions. We found that the responses of *E. huxleyi* to one-day versus  
577 two-day temperature variations were different at both low and high temperature. For  
578 instance, under low temperature the transition from the warm phase to the cool phase  
579 during the thermal variation could be treated as a low temperature stress leading to a  
580 lag phase in growth. The growth rate of the one-day variation treatment at the cool  
581 phase was lower than that of the two-day variation, suggesting that physiological  
582 acclimation is not rapid enough to accommodate to the shorter variation treatment,  
583 while the two day variation allows enough time for growth to recover. However, at  
584 the warm phase (21 °C) there was no difference in growth rates between the one-day  
585 and two-day variations compared with the constant 21-degree treatment. These  
586 results imply that there was a shorter lag phase after transfer at the optimal  
587 temperature point (21 °C at the warm phase) than during low temperature stress (16  
588 °C at the cool phase).

589 There was no significant difference in photosynthetic rates between the one-day

590 and two-day variation during the warm phase (21 °C), but both were higher than  
591 during the cool phase, indicating the photosynthetic rate was correlated to the  
592 thermal variation cycle. However, for the calcification rate there was no significant  
593 difference between one-day and two-day variations during either the cool or warm  
594 phases. These results suggested that photosynthesis was more responsive to  
595 temperature variations than calcification, and so ultimately determined the growth  
596 rate in both cool and warm phases. Feng et al. (2017) reported a similar relationship  
597 between growth and photosynthetic rates of a Southern Hemisphere cultured at  
598 different temperatures.

599 Temperature variation frequencies also strongly influenced elemental  
600 composition. In low temperature experiments, the cellular contents of PON, POP and  
601 POC in the one-day variation treatment were all higher than under two-day  
602 variations. A notable exception to this trend was the cellular PIC content, which was  
603 not significantly different between one-day and two-day variation treatments. The  
604 PIC content was positively correlated to calcification and relatively stable, indicating  
605 that coccolith production and storage of *E. huxleyi* was relatively independent of the  
606 frequency of thermal variation.

607 Unlike the photosynthetic rate, the cellular elemental content of one-day and  
608 two-day variations were significantly different, but were not changed during  
609 temperature variation when transitioning from the warm phase to the cool phase or  
610 vice versa. The temperature dependent photosynthetic enzyme activity likely  
611 determined the similar photosynthetic rate of one-day and two-day variation

612 treatments at both cool and warm phase in our short-term experiment, but the  
613 divergent responses of cellular stoichiometry in one-day and two-day thermal  
614 variations indicated different mechanisms of rapid acclimation to different thermal  
615 fluctuation frequencies. Our results imply that the responses of *E. huxleyi* to one-day  
616 and two-day thermal variations have different patterns, but both reach stable states  
617 during extended periods of temperature fluctuation. Due to decreasing POC content,  
618 the PIC/POC ratio increased in the two-day variation compared with the one-day  
619 variation, suggesting that more rapid thermal fluctuations might lead to a decrease in  
620 calcite ballasting of sinking organic carbon.

621 Under the high temperature scenario, thermal variation forces the microalgae to  
622 intermittently deal with a lethal high temperature during the warm phase (28 °C),  
623 with potentially irreversible damage to the cells. In the “summer” experiments, the  
624 mean growth rate of the two-day variation was much lower than that of the one-day  
625 variation. This mainly resulted from the negative growth rate of two-day variation  
626 cultures during the warm phase (28 °C), whereas the growth rate of the one-day  
627 variation was  $>0.20 \text{ d}^{-1}$ . This result demonstrates that high frequency temperature  
628 variations (one-day) can partly mitigate growth inhibition by high temperatures in *E.*  
629 *huxleyi*, and so allow tolerance to extreme thermal events relative to longer  
630 exposures. This observation agrees with previous studies of other marine organisms  
631 such as corals (Oliver & Palumbi, 2011; Safaie et al., 2018). In the case of our  
632 experiments, the lag phase and metabolic inertia would help to maintain the  
633 microalgae during short exposures (one-day) to high temperature when transitioning

634 from the cool phase (23 °C) to the warm phase (28 °C).

635 Likewise, the particulate organic element contents (PON, POP and POC) of *E.*  
636 *huxleyi* were more stable in one-day than in two-day temperature variation treatments.  
637 The relatively steady status of cellular particulate organic matter content in the high  
638 frequency temperature variation treatment may conserve energy, compared to the  
639 energy-intensive redistribution of major cellular components under lower frequency  
640 temperature variations. This differential energetic cost may help to explain the  
641 differences in growth rates between the two treatments. Adaptation to high  
642 temperature may also require higher investment in repair machinery, such as heat  
643 shock proteins, leading to an increased demand for nitrogen and other nutrients, thus  
644 increasing cellular POC, PON and POP contents (O'Donnell et al., 2018).

#### 645 **Prediction and modelling of *E. huxleyi* responses to thermal variation**

646 Mathematical curves based on population growth rates from laboratory studies  
647 have been used to predict future population abundance, persistence or fitness in a  
648 changing world (Bernhardt et al., 2018; Deutsch et al., 2008; Jiang et al. 2017). We  
649 applied a modified version of the Eppley thermal performance curve model with the  
650 addition of non-linear averaging (Bernhardt et al., 2018) to predict the influence of  
651 thermal variation on the growth rate of *E. huxleyi* (Fig. 8). *E. huxleyi* growth rates  
652 were predicted to be much lower at warmer temperatures under variable conditions  
653 compared to constant conditions, but there were no significant differences at cooler  
654 temperatures. Thus, the effect of thermal variation on population growth at the upper  
655 thermal limit was predicted to be stronger than that in the lower portion of the thermal

656 range (Bernhardt et al., 2018; Sunday et al., 2012). This phenomenon has been widely  
657 observed in **ectothermic animal taxa** (Dell et al., 2011), but this model for the effect of  
658 thermal variation on population growth rate may lack the ability to predict species  
659 responses at the extreme edges of their ranges (Bernhardt et al., 2018).

660 Our results showed that the measured effects of a variable thermal regime on *E.*  
661 *huxleyi* growth rate fitted well with model-predicted values at a relatively low  
662 temperature (mean=18.5 °C), but differed considerably at high temperature  
663 (mean=25.5 °C). This was especially evident under the two-day variation conditions  
664 at a mean of 25.5 °C, where the growth rate was sharply lower than predicted from the  
665 constant **temperature performance curve**-based model. This result suggests that  
666 transient heat waves may erode thermal tolerances of *E. huxleyi* populations already  
667 growing near their upper thermal limits, and that the frequency and duration of such  
668 extreme events is critically important in determining the magnitude of this stress. **Qu**  
669 **et al. (2019) reported that the tropical cyanobacterium *Trichodesmium erythraeum***  
670 **only showed a slight decrease of growth rate with thermal variation treatments at high**  
671 **temperature (average 30°C), compared with constant 30°C treatments. In contrast, the**  
672 **sensitivity of *E. huxleyi* to increasing thermal variability may reduce its fitness and its**  
673 **ability to compete with other taxa such as diatoms and cyanobacteria in the future**  
674 **ocean.**

675 Although thermal variation at high temperature negatively impacted the growth  
676 rate of *E. huxleyi* in our experiment, our relatively short-term study didn't address the  
677 potential for *E. huxleyi* to evolve under selection by frequent extreme heat events.

678 Evolutionary change in the thermal optimum and the maximum growth temperature in  
679 response to ocean warming may reduce heat-induced mortality, and mitigate some  
680 ecological impacts of global warming (O'Donnell et al., 2018, Thomas et al., 2012).  
681 For example, Schlüter et al. (2014) found that after one year of experimental  
682 adaptation to warming (26.3°C), the marine coccolithophore *E. huxleyi* evolved a  
683 higher growth rate when assayed at the upper thermal tolerance limit. Similar results  
684 were reported for the marine diatom *Thalassiosira pseudonana* in recent studies  
685 (O'Donnell et al., 2018; Schaum et al., 2018). Schaum et al. (2018) also found that the  
686 evolution of thermal tolerance in marine diatoms can be particularly rapid in  
687 fluctuating environments. Furthermore, populations originating from more variable  
688 environments are generally more plastic (Schaum & Collins, 2014; Schaum et al.,  
689 2013). Long-term evolutionary experiments with *E. huxleyi* will be necessary to  
690 determine how the thermal performance curve of this important marine calcifier may  
691 diverge under selection by different frequencies and durations of extreme thermal  
692 variation events.

693 Understanding the combination of ocean warming and magnified thermal  
694 variability may be a prerequisite to accurately predicting the effects of climate change  
695 on the growth and physiology of the key marine calcifier *E. huxleyi*. This information  
696 will help to inform biogeochemical models of the marine and global carbon cycles,  
697 and ecological models of phytoplankton distributions and primary productivity. How  
698 changing thermal variation frequencies and heat wave events will affect marine  
699 phytoplankton remains a relatively under-explored topic, but one that is likely to

700 become increasingly important in the future changing ocean.

701

702 **Acknowledgements**

703 Support was provided by the U.S. National Science Foundation Biological  
704 Oceanography grants OCE1538525 and OCE1638804 to F-XF and DAH, National  
705 Key Research and Development Program of China 2016YFA0601302 to Y-HG.  
706 X-WW was supported by a grant from the China Scholarship Council.

707

708 **References**

- 709 Bernhardt, J. R., Sunday, J. M., Thompson, P. L., and O'Connor, M. I.: Nonlinear  
710 averaging of thermal experience predicts population growth rates in a thermally  
711 variable environment, *bioRxiv*, 247908, 2018.
- 712 Boyce, D. G., Lewis, M. R., and Worm, B.: Global phytoplankton decline over the  
713 past century, *Nature*, 466, 591, 2010.
- 714 Boyd, P., Dillingham, P., McGraw, C., Armstrong, E., Cornwall, C., Feng, Y.-y., Hurd,  
715 C., Gault-Ringold, M., Roleda, M., and Timmins-Schiffman, E.: Physiological  
716 responses of a Southern Ocean diatom to complex future ocean conditions,  
717 *Nature Climate Change*, 6, 207-216, <https://doi.org/10.1038/nclimate2811>, 2015.
- 718 Boyd, P. W., Strzepek, R., Fu, F., and Hutchins, D. A.: Environmental control of open-  
719 ocean phytoplankton groups: Now and in the future, *Limnol. Oceanogr.*, 55,  
720 1353-1376, <https://doi.org/10.4319/lo.2010.55.3.1353>, 2010.
- 721 Boyd, P. W., Collins, S., Dupont, S., Fabricius, K., Gattuso, J. P., Havenhand, J.,  
722 Hutchins, D. A., Riebesell, U., Rintoul, M. S., and Vichi, M.: Experimental  
723 strategies to assess the biological ramifications of multiple drivers of global  
724 ocean change—A review, *Glob. Chang. Biol.*, 24, 2239-2261, <https://doi.org/10.1111/gcb.14102>, 2018.
- 726 Bozinovic, F., Bastías, D. A., Boher, F., Clavijo-Baquet, S., Estay, S. A., and  
727 Angilletta Jr, M. J.: The mean and variance of environmental temperature  
728 interact to determine physiological tolerance and fitness, *Physiol. Biochem.  
729 Zool.*, 84, 543-552, <https://doi.org/10.1086/662551>, 2011.

730 Buitenhuis, E. T., Pangerc, T., Franklin, D. J., Le Quéré, C., and Malin, G.: Growth  
731 rates of six coccolithophorid strains as a function of temperature, *Limnol.*  
732 *Oceanogr.*, 53, 1181-1185, [https://doi.org/ 10.4319/lo.2008.53.3.1181](https://doi.org/10.4319/lo.2008.53.3.1181), 2008.

733 Burgmer, T., and Hillebrand, H.: Temperature mean and variance alter phytoplankton  
734 biomass and biodiversity in a long-term microcosm experiment, *Oikos*, 120,  
735 922-933, <https://doi.org/2011>.

736 Cáceres, C. E.: Temporal variation, dormancy, and coexistence: a field test of the  
737 storage effect, *Proceedings of the National Academy of Sciences*, 94, 9171-9175,  
738 [https://doi.org/ 10.2307/42576](https://doi.org/10.2307/42576), 1997.

739 De Bodt, C., Van Oostende, N., Harlay, J., Sabbe, K., and Chou, L.: Individual and  
740 interacting effects of pCO<sub>2</sub> and temperature on *Emiliana huxleyi* calcification:  
741 study of the calcite production, the coccolith morphology and the coccosphere  
742 size, *Biogeosciences*, 7, 1401-1412, [https://doi.org/ 10.5194/bg-7-1401-2010](https://doi.org/10.5194/bg-7-1401-2010),  
743 2010.

744 Dell, A. I., Pawar, S., and Savage, V. M.: Systematic variation in the temperature  
745 dependence of physiological and ecological traits, *Proceedings of the National*  
746 *Academy of Sciences*, 108, 10591-10596, [https://doi.org/ 10.2307/27978658](https://doi.org/10.2307/27978658),  
747 2011.

748 Deutsch, C. A., Tewksbury, J. J., Huey, R. B., Sheldon, K. S., Ghalambor, C. K., Haak,  
749 D. C., and Martin, P. R.: Impacts of climate warming on terrestrial ectotherms  
750 across latitude, *Proceedings of the National Academy of Sciences*, 105,  
751 6668-6672, [https://doi.org/ 10.1073/pnas.0709472105](https://doi.org/10.1073/pnas.0709472105), 2008.

752 Eppley, R. W.: Temperature and phytoplankton growth in the sea, *Fish. bull.*, 70,  
753 1063-1085, 1972.

754 Feng, Y., Warner, M. E., Zhang, Y., Sun, J., Fu, F.-X., Rose, J. M., and Hutchins, D. A.:  
755 Interactive effects of increased pCO<sub>2</sub>, temperature and irradiance on the marine  
756 coccolithophore *Emiliana huxleyi* (Prymnesiophyceae), *Eur. J. Phycol.*, 43,  
757 87-98, <https://doi.org/10.1080/09670260701664674>, 2008.

758 Feng, Y., Roleda, M. Y., Armstrong, E., Boyd, P. W., and Hurd, C. L.: Environmental  
759 controls on the growth, photosynthetic and calcification rates of a Southern  
760 Hemisphere strain of the coccolithophore *Emiliana huxleyi*, *Limnol. Oceanogr.*,  
761 62, 519-540, <https://doi.org/10.1002/lno.10442>, 2017.

762 Feng, Y., Roleda, M. Y., Armstrong, E., Law, C. S., Boyd, P. W., and Hurd, C. L.:  
763 Environmental controls on the elemental composition of a Southern Hemisphere  
764 strain of the coccolithophore *Emiliana huxleyi*, *Biogeosciences*, 15, 581-595,  
765 <https://doi.org/10.1002/lno.10442>, 2018.

766 Friedland, K. D., Mouw, C. B., Asch, R. G., Ferreira, A. S. A., Henson, S., Hyde, K. J.,  
767 Morse, R. E., Thomas, A. C., and Brady, D. C.: Phenology and time series trends  
768 of the dominant seasonal phytoplankton bloom across global scales, *Global Ecol.*  
769 *Biogeogr.*, 27, 551-569, <https://doi.org/10.1111/geb.12717>, 2018.

770 Fu, F.-X., Yu, E., Garcia, N. S., Gale, J., Luo, Y., Webb, E. A., and Hutchins, D. A.:  
771 Differing responses of marine N<sub>2</sub> fixers to warming and consequences for future  
772 diazotroph community structure, *Aquat. Microb. Ecol.*, 72, 33-46, [https://doi.org/](https://doi.org/10.5194/bgd-12-4273-2015)  
773 [10.5194/bgd-12-4273-2015](https://doi.org/10.5194/bgd-12-4273-2015), 2014.

774 Fu F.-X., Tatters A.O., and Hutchins, D.A.: Global change and the future of harmful  
775 algal blooms in the ocean. *Marine Ecology Progress Series* 470: 207-233 DOI:  
776 10.3354/meps10047, 2012.

777 Fu, F. X., Warner, M. E., Zhang, Y., Feng, Y., and Hutchins, D. A.: Effects of  
778 increased temperature and CO<sub>2</sub> on photosynthesis, growth, and elemental ratios  
779 in marine *Synechococcus* and *Prochlorococcus* (Cyanobacteria), *J. Phycol.*, 43,  
780 485-496, [https://doi.org/ 10.1111/j.1529-8817.2007.00355.x](https://doi.org/10.1111/j.1529-8817.2007.00355.x), 2007.

781 Gao, K., Zhang, Y., and Häder, D.-P.: Individual and interactive effects of ocean  
782 acidification, global warming, and UV radiation on phytoplankton, *J. Appl.*  
783 *Phycol.*, 30, 743-759, [https://doi.org/ 10.1007/s10811-017-1329-6](https://doi.org/10.1007/s10811-017-1329-6), 2018.

784 Gerecht, A. C., Šupraha, L., Edvardsen, B., Probert, I., and Henderiks, J.: High  
785 temperature decreases the PIC/POC ratio and increases phosphorus requirements  
786 in *Coccolithus pelagicus* (Haptophyta), *Biogeosciences*, 11, 3531-3545,  
787 [https://doi.org/ 10.5194/bg-11-3531-2014](https://doi.org/10.5194/bg-11-3531-2014), 2014.

788 Gobler, C. J., Doherty, O. M., Hattenrath-Lehmann, T. K., Griffith, A. W., Kang, Y.,  
789 and Litaker, R. W.: Ocean warming since 1982 has expanded the niche of toxic  
790 algal blooms in the North Atlantic and North Pacific oceans, *Proceedings of the*  
791 *National Academy of Sciences*, 201619575, [https://doi.org/](https://doi.org/10.1073/pnas.1619575114)  
792 [10.1073/pnas.1619575114](https://doi.org/10.1073/pnas.1619575114), 2017.

793 Hallegraeff, G. M.: Ocean climate change, phytoplankton community responses, and  
794 harmful algal blooms: a formidable predictive challenge, *J. Phycol.*, 46, 220-235,  
795 [https://doi.org/ 10.1111/j.1529-8817.2010.00815.x](https://doi.org/10.1111/j.1529-8817.2010.00815.x), 2010.

796 Hare, C. E., Leblanc, K., Ditullio, G. R., Kudela, R. M., Zhang, Y., Lee, P. A.,  
797 Riseman, S., and Hutchins, D. A.: Consequences of increased temperature and  
798 CO<sub>2</sub> for phytoplankton community structure in the Bering Sea, *Marine Ecology*  
799 *Progress*, 352, 9-16, <https://doi.org/10.3354/meps07182>, 2007.

800 Holligan, P., Viollier, M., Harbour, D., Camus, P., and Champagne-Philippe, M.:  
801 Satellite and ship studies of coccolithophore production along a continental shelf  
802 edge, *Nature*, 304, 339, <https://doi.org/10.1038/304339a0>, 1983.

803 Holligan, P. M., Fernández, E., Aiken, J., Balch, W. M., Boyd, P., Burkill, P. H., Finch,  
804 M., Groom, S. B., Malin, G., and Muller, K.: A biogeochemical study of the  
805 coccolithophore, *Emiliana huxleyi*, in the North Atlantic, *Global Biogeochem.*  
806 *Cycles*, 7, 879-900, <https://doi.org/10.1029/93GB01731>, 1993.

807 Hoppe, C., Langer, G., and Rost, B.: *Emiliana huxleyi* shows identical responses to  
808 elevated pCO<sub>2</sub> in TA and DIC manipulations, *J. Exp. Mar. Bio. Ecol.*, 406, 54-62,  
809 <https://doi.org/10.1016/j.jembe.2011.06.008>, 2011.

810 Hutchins, D. A., Ditullio, G. R., Zhang, Y., and Bruland, K. W.: An iron limitation  
811 mosaic in the California upwelling regime, *Limnology & Oceanography*, 43,  
812 1037-1054, 1998.

813 Hutchins, D. A., and Fu, F.: Microorganisms and ocean global change, *Nat Microbiol*,  
814 2, 17058, <https://doi.org/10.1038/nmicrobiol.2017.58>, 2017.

815 Iglesias-Rodríguez, M. D., Brown, C. W., Doney, S. C., Kleypas, J., Kolber, D.,  
816 Kolber, Z., Hayes, P. K., and Falkowski, P. G.: Representing key phytoplankton  
817 functional groups in ocean carbon cycle models: Coccolithophorids, *Global*

818 Biogeochem. Cycles, 16, 47-41-47-20, [https://doi.org/ 10.1029/2001GB001454](https://doi.org/10.1029/2001GB001454),  
819 2002.

820 Jiang, L., Sun, Y.-F., Zhang, Y.-Y., Zhou, G.-W., Li, X.-B., McCook, L. J., Lian, J.-S.,  
821 Lei, X.-M., Liu, S., and Cai, L.: Impact of diurnal temperature fluctuations on  
822 larval settlement and growth of the reef coral *Pocillopora damicornis*,  
823 Biogeosciences, 14, 5741-5752, [https://doi.org/ 10.5194/bg-14-5741-2017](https://doi.org/10.5194/bg-14-5741-2017), 2017.

824 Keys, M., Tilstone, G., Findlay, H. S., Widdicombe, C. E., and Lawson, T.: Effects of  
825 elevated CO<sub>2</sub> and temperature on phytoplankton community biomass, species  
826 composition and photosynthesis during an experimentally induced autumn bloom  
827 in the western English Channel, Biogeosciences, 15, 3203-3222, [https://doi.org/](https://doi.org/10.5194/bg-15-3203-2018)  
828 [10.5194/bg-15-3203-2018](https://doi.org/10.5194/bg-15-3203-2018), 2018.

829 Klaas, C., and Archer, D. E.: Association of sinking organic matter with various types  
830 of mineral ballast in the deep sea: Implications for the rain ratio, Global  
831 Biogeochem. Cycles, 16, 63-61-63-14, [https://doi.org/ 10.1029/2001GB001765](https://doi.org/10.1029/2001GB001765),  
832 2002.

833 Kling, J.D., Lee, M.D., Fu, F.-X., Phan, M., Wang, X., Qu, P.P., and Hutchins, D.A.:  
834 Transient exposure to novel high temperatures reshapes coastal phytoplankton  
835 communities. *ISME Journal*, in press.

836 Kremer, C. T., Fey, S. B., Arellano, A. A., and Vasseur, D. A.: Gradual plasticity alters  
837 population dynamics in variable environments: thermal acclimation in the green  
838 alga *Chlamydomonas reinhardtii*, Proceedings Biological Sciences, 285,  
839 20171942, [https://doi.org/ 10.1098/rspb.2017.1942](https://doi.org/10.1098/rspb.2017.1942), 2018.

840 Krumhardt, K. M., Lovenduski, N. S., Iglesias-Rodriguez, M. D., and Kleypas, J. A.:  
841 Coccolithophore growth and calcification in a changing ocean, *Prog. Oceanogr.*,  
842 159, 276-295, [https://doi.org/ 10.1016/j.pocean.2017.10.007](https://doi.org/10.1016/j.pocean.2017.10.007), 2017.

843 Matson, P. G., Ladd, T. M., Halewood, E. R., Sangodkar, R. P., Chmelka, B. F., and  
844 Iglesias-Rodriguez, M. D.: Intraspecific differences in biogeochemical responses  
845 to thermal change in the coccolithophore *Emiliana huxleyi*, *PLoS One*, 11,  
846 e0162313, <https://doi.org/10.1371/journal.pone.0162313>, 2016.

847 Monteiro, F. M., Bach, L. T., Brownlee, C., Bown, P., Rickaby, R. E., Poulton, A. J.,  
848 Tyrrell, T., Beaufort, L., Dutkiewicz, S., and Gibbs, S.: Why marine  
849 phytoplankton calcify, *Science Advances*, 2, e1501822, [https://doi.org/](https://doi.org/10.1126/sciadv.1501822)  
850 [10.1126/sciadv.1501822](https://doi.org/10.1126/sciadv.1501822), 2016.

851 Morán, X. A. G., LÓPEZ-URRUTIA, Á., CALVO-DÍAZ, A., and Li, W. K.:  
852 Increasing importance of small phytoplankton in a warmer ocean, *Glob. Chang.*  
853 *Biol.*, 16, 1137-1144, [https://doi.org/ 10.1111/j.1365-2486.2009.01960.x](https://doi.org/10.1111/j.1365-2486.2009.01960.x), 2010.

854 Neukermans, G., Oziel, L., and Babin, M.: Increased intrusion of warming Atlantic  
855 water leads to rapid expansion of temperate phytoplankton in the Arctic, *Glob.*  
856 *Chang. Biol.*, [https://doi.org/ 10.1111/gcb.14075](https://doi.org/10.1111/gcb.14075), 2018.

857 Norberg, J.: Biodiversity and ecosystem functioning: a complex adaptive systems  
858 approach, *Limnol. Oceanogr.*, 49, 1269-1277, [https://doi.org/](https://doi.org/10.4319/lo.2004.49.4_part_2.1269)  
859 [10.4319/lo.2004.49.4\\_part\\_2.1269](https://doi.org/10.4319/lo.2004.49.4_part_2.1269), 2004.

860 O'Donnell, D. R., Hamman, C. R., Johnson, E. C., Kremer, C. T., Klausmeier, C. A.,  
861 and Litchman, E.: Rapid thermal adaptation in a marine diatom reveals

862 constraints and tradeoffs, *Glob. Chang. Biol.*, doi:10.1111/gcb.14360, 2018.

863 Oliver, T., and Palumbi, S.: Do fluctuating temperature environments elevate coral  
864 thermal tolerance?, *Coral Reefs*, 30, 429-440, [https://doi.org/](https://doi.org/10.1007/s00338-011-0721-y)  
865 10.1007/s00338-011-0721-y, 2011.

866 Paasche, E.: Reduced coccolith calcite production under light-limited growth: a  
867 comparative study of three clones of *Emiliana huxleyi* (Prymnesiophyceae),  
868 *Phycologia*, 38, 508-516, 1999.

869 Paasche, E.: A review of the coccolithophorid *Emiliana huxleyi* (Prymnesiophyceae),  
870 with particular reference to growth, coccolith formation, and  
871 calcification-photosynthesis interactions, *Phycologia*, 40, 503-529,  
872 [https://doi.org/ 10.2216/i0031-8884-40-6-503.1](https://doi.org/10.2216/i0031-8884-40-6-503.1), 2001.

873 Platt, T., Gallegos, C. L., & Harrison, W. G.: Photoinhibition of photosynthesis in  
874 natural assemblages of marine-phytoplankton. *Journal of Marine Research*, 38(4),  
875 687-701, 1980.

876 Qu, P., Fu, F.-X., Kling, J. D., Huh, M., Wang, X., and Hutchins, D. A.: Distinct  
877 responses of the nitrogen-fixing marine cyanobacterium *Trichodesmium* to a  
878 thermally variable environment as a function of phosphorus availability,  
879 *Frontiers in Microbiology*, 10, 10.3389/fmicb.2019.01282, 2019.

880 Rasconi, S., Winter, K., and Kainz, M. J.: Temperature increase and fluctuation induce  
881 phytoplankton biodiversity loss—Evidence from a multi-seasonal mesocosm  
882 experiment, *Ecology and evolution*, 7, 2936-2946, [https://doi.org/](https://doi.org/10.1002/ece3.2889)  
883 10.1002/ece3.2889, 2017.

884 Raven, J. A., and Crawford, K.: Environmental controls on coccolithophore  
885 calcification, *Mar. Ecol. Prog. Ser.*, 470, 137-166, [https://doi.org/](https://doi.org/10.3354/meps09993)  
886 [10.3354/meps09993](https://doi.org/10.3354/meps09993), 2012.

887 Riegman, R., Stolte, W., Noordeloos, A. A., and Slezak, D.: Nutrient uptake and  
888 alkaline phosphatase (EC 3: 1: 3: 1) activity of *Emiliania huxleyi*  
889 (Prymnesiophyceae) during growth under N and P limitation in continuous  
890 cultures, *J. Phycol.*, 36, 87-96, [https://doi.org/](https://doi.org/10.1046/j.1529-8817.2000.99023.x)  
891 [10.1046/j.1529-8817.2000.99023.x](https://doi.org/10.1046/j.1529-8817.2000.99023.x), 2000.

892 Rosas-Navarro, A., Langer, G., and Ziveri, P.: Temperature affects the morphology  
893 and calcification of *Emiliania huxleyi* strains, *Biogeosciences*, 13, 2913-2926,  
894 <https://doi.org/10.5194/bg-13-2913-2016>, 2016.

895 Safaie, A., Silbiger, N. J., McClanahan, T. R., Pawlak, G., Barshis, D. J., Hench, J. L.,  
896 Rogers, J. S., Williams, G. J., and Davis, K. A.: High frequency temperature  
897 variability reduces the risk of coral bleaching, *Nat Commun*, 9, [https://doi.org/](https://doi.org/10.1038/s41467-018-04074-2)  
898 [10.1038/s41467-018-04074-2](https://doi.org/10.1038/s41467-018-04074-2), 2018.

899 Schaum, C. E., and Collins, S.: Plasticity predicts evolution in a marine alga,  
900 *Proceedings of the Royal Society B: Biological Sciences*, 281, 20141486,  
901 <https://doi.org/10.1098/rspb.2014.1486>, 2014.

902 Schaum, C. E., Buckling, A., Smirnoff, N., Studholme, D., and Yvondurocher, G.:  
903 Environmental fluctuations accelerate molecular evolution of thermal tolerance  
904 in a marine diatom, *Nat Commun*, 9, 1719, [https://doi.org/](https://doi.org/10.1038/s41467-018-03906-5)  
905 [10.1038/s41467-018-03906-5](https://doi.org/10.1038/s41467-018-03906-5), 2018.

906 Schaum, E., Rost, B., Millar, A. J., and Collins, S.: Variation in plastic responses of a  
907 globally distributed picoplankton species to ocean acidification, *Nature Climate*  
908 *Change*, 3, 298-302, <https://doi.org/10.1038/NCLIMATE1774>, 2013.

909 Schlüter, L., Kai, T. L., Gutowska, M. A., Gröger, J. P., Riebesell, U., and Reusch, T.  
910 B. H.: Adaptation of a globally important coccolithophore to ocean warming and  
911 acidification, *Nature Climate Change*, 4, 1024-1030, [https://doi.org/](https://doi.org/10.1038/nclimate2379)  
912 [10.1038/nclimate2379](https://doi.org/10.1038/nclimate2379), 2014.

913 Sett, S., Bach, L. T., Schulz, K. G., Koch-Klavsen, S., Lebrato, M., and Riebesell, U.:  
914 Temperature modulates coccolithophorid sensitivity of growth, photosynthesis  
915 and calcification to increasing seawater pCO<sub>2</sub>, *PLoS One*, 9, e88308,  
916 <https://doi.org/10.1371/journal.pone.0088308>, 2014.

917 Shurin, J. B., Winder, M., Adrian, R., Keller, W., Matthews, B., Paterson, A. M.,  
918 Paterson, M. J., Pinel-Alloul, B., Rusak, J. A., and Yan, N. D.: Environmental  
919 stability and lake zooplankton diversity—contrasting effects of chemical and  
920 thermal variability, *Ecol. Lett.*, 13, 453-463, [https://doi.org/](https://doi.org/10.1111/j.1461-0248.2009.01438.x)  
921 [10.1111/j.1461-0248.2009.01438.x](https://doi.org/10.1111/j.1461-0248.2009.01438.x), 2010.

922 Solórzano, L., and Sharp, J. H.: Determination of total dissolved phosphorus and  
923 particulate phosphorus in natural waters, *Limnology & Oceanography*, 25,  
924 754-758, 1980.

925 Sunda, W. G., Price, N. M., and Morel, F. M.: Trace metal ion buffers and their use in  
926 culture studies, *Algal culturing techniques*, 4, 35-63, 2005.

927 Sunday, J. M., Bates, A. E., and Dulvy, N. K.: Thermal tolerance and the global

928 redistribution of animals, *Nature Climate Change*, 2, 686, [https://doi.org/](https://doi.org/10.1038/nclimate1539)  
929 10.1038/nclimate1539, 2012.

930 Tatters, A. O., Schnetzer, A., Xu, K., Walworth, N. G., Fu, F., Spackeen, J. L., Sipler,  
931 R. E., Bertrand, E. M., McQuaid, J. B., and Allen, A. E.: Interactive effects of  
932 temperature, CO<sub>2</sub> and nitrogen source on a coastal California diatom assemblage,  
933 *J. Plankton Res.*, 40, 151-164, 2018.

934 Thomas, M. K., Kremer, C. T., Klausmeier, C. A., and Litchman, E.: A global pattern  
935 of thermal adaptation in marine phytoplankton, *Science*, 338, 1085-1088,  
936 [https://doi.org/ 10.1126/science.1224836](https://doi.org/10.1126/science.1224836), 2012.

937 Vázquez, D. P., Gianoli, E., Morris, W. F., and Bozinovic, F.: Ecological and  
938 evolutionary impacts of changing climatic variability, *Biological Reviews*, 92,  
939 22-42, [https://doi.org/ 10.1111/brv.12216](https://doi.org/10.1111/brv.12216), 2017.

940 Vasseur, D. A., DeLong, J. P., Gilbert, B., Greig, H. S., Harley, C. D., McCann, K. S.,  
941 Savage, V., Tunney, T. D., and O'Connor, M. I.: Increased temperature variation  
942 poses a greater risk to species than climate warming, *Proceedings of the Royal*  
943 *Society of London B: Biological Sciences*, 281, 20132612, [https://doi.org/](https://doi.org/10.1098/rspb.2013.2612)  
944 10.1098/rspb.2013.2612, 2014.

945 Westbroek, P., Brown, C. W., van Bleijswijk, J., Brownlee, C., Brummer, G. J., Conte,  
946 M., Egge, J., Fernández, E., Jordan, R., and Knappertsbusch, M.: A model  
947 system approach to biological climate forcing. The example of *Emiliana huxleyi*,  
948 *Global Planet. Change*, 8, 27-46, 1993.

949 Yvon-Durocher, G., Allen, A. P., Cellamare, M., Dossena, M., Gaston, K. J., Leitaó,

950 M., Montoya, J. M., Reuman, D. C., Woodward, G., and Trimmer, M.: Five years  
951 of experimental warming increases the biodiversity and productivity of  
952 phytoplankton, PLoS Biol., 13, e1002324, [https://doi.org/](https://doi.org/10.1371/journal.pbio.1002324)  
953 10.1371/journal.pbio.10023242015.

954 Zander, A., Bersier, L. F., and Gray, S. M.: Effects of temperature variability on  
955 community structure in a natural microbial food web, Glob. Chang. Biol., 23,  
956 56-67, <https://doi.org/10.1111/gcb.13374>, 2017.

957 Zhang, M., Qin, B., Yu, Y., Yang, Z., Shi, X., and Kong, F.: Effects of temperature  
958 fluctuation on the development of cyanobacterial dominance in spring:  
959 Implication of future climate change, Hydrobiologia, 763, 135-146,  
960 <https://doi.org/10.1007/s10750-015-2368-0>, 2016.

961 Zhang, Y., Klapper, R., Lohbeck, K. T., Bach, L. T., Schulz, K. G., Reusch, T. B. H.,  
962 and Riebesell, U.: Between- and within-population variations in thermal reaction  
963 norms of the coccolithophore *Emiliana huxleyi*, Limnol. Oceanogr., 59,  
964 1570-1580, [10.4319/lo.2014.59.5.1570](https://doi.org/10.4319/lo.2014.59.5.1570), 2014.

965 Zhu, Z., Qu, P., Fu, F., Tennenbaum, N., Tatters, A. O., and Hutchins, D. A.:  
966 Understanding the blob bloom: Warming increases toxicity and abundance of the  
967 harmful bloom diatom *Pseudo-nitzschia* in California coastal waters, Harmful  
968 Algae, 67, 36-43, <https://doi.org/10.1016/j.hal.2017.06.004>, 2017.

969

970

971

972 **Figure legends:**

973 **Fig. 1** Thermal performance curve showing cell-specific growth rates ( $d^{-1}$ ) of  
974 *Emiliana huxleyi* CCMP371 across a temperature range from 8.5 to 28.6 °C. Symbols  
975 represent means and error bars are the standard deviations of three replicates at each  
976 temperature, but in many cases the errors bars are smaller than the symbols.

977 **Fig. 2** Changes in *Emiliana huxleyi* TPC/PON ratios (**A**), POC/PON ratios (**B**),  
978 PIC/POC ratios (**C**) and Cha/POC ratios (**D**) across a temperature range from 8.5 to  
979 28.6 °C. Dashed lines represent the average ratios for the entire temperature range.  
980 Bars represent means and error bars are the standard deviations of three replicates at  
981 each temperature. Symbols \* represent the significant difference ( $p < 0.05$ ) between  
982 average ratios and the ratio at each temperature.

983 **Fig. 3** *Emiliana huxleyi* growth rate responses to constant temperatures, and during  
984 the warm and cool phases of the two thermal variation frequencies (one-day and  
985 two-day), under low (**A**) and high (**B**) mean temperatures. The thick black line in the  
986 boxplots represent median values for each experimental treatment; whiskers on  
987 boxplots indicate  $1.5 \times$  interquartile range. Listed p-values with their respective  
988 brackets are the statistical significance between two treatments.

989 **Fig. 4** Responses of *Emiliana huxleyi* PIC/POC ratios to constant temperatures, and  
990 during the warm and cool phases of two thermal variation frequencies (one-day and  
991 two-day), under low (**A**) and high (**B**) mean temperatures. LT: Low temperature; HT:  
992 High temperature. The thick black line in the boxplots represent median values for  
993 each experimental treatment; whiskers on boxplots indicate  $1.5 \times$  interquartile range.

994 Listed p-values with their respective brackets denote the statistical significance  
995 between two treatments.

996 **Fig. 5** Responses of *Emiliana huxleyi* photosynthetic carbon fixation and  
997 calcification at constant temperatures and during the warm and cool phases of two  
998 thermal variation frequencies (one-day and two-day), including: total carbon fixation  
999 (photosynthesis + calcification) at low (**A**) and high (**B**) temperatures; photosynthetic  
1000 carbon fixation at low (**C**) and high (**D**) temperatures; and calcification rates at low (**E**)  
1001 and high (**F**) temperatures. LT: Low temperature; HT: High temperature. The thick  
1002 black line in the boxplots represent median values for each experimental treatment;  
1003 whiskers on boxplots indicate  $1.5 \times$  interquartile range. Listed p-values with their  
1004 respective brackets denote the statistical significance between two treatments.

1005 **Fig. 6** Responses of *Emiliana huxleyi* calcification to photosynthesis ratios (cal/photo)  
1006 to constant temperatures, and during the warm and cool phases of two thermal  
1007 variation frequencies (1 day and 2 day), under low (**A**) and high (**B**) mean  
1008 temperatures. LT: Low temperature; HT: High temperature. The thick black line in the  
1009 boxplots represent median values for each experimental treatment; whiskers on  
1010 boxplots indicate  $1.5 \times$  interquartile range. Listed p-values with their respective  
1011 brackets denote the statistical significance between two treatments.

1012 **Fig. 7** Responses of *Emiliana huxleyi* elemental ratios in two thermal variation  
1013 frequency treatments (1 day and 2 day) compared to constant temperatures, for:  
1014 TPC/PON (**A**, cool phase and **B**, warm phase), PON/POP (**C**, cool phase and **D**, warm  
1015 phase) and Chl *a*/POC ratios (**E**, cool phase and **F**, warm phase). LT: Low temperature;

1016 HT: High temperature. The thick black line in the boxplots represent median values  
1017 for each experimental treatment; whiskers on boxplots indicate  $1.5 \times$  interquartile  
1018 range. Listed p-values with their respective brackets denote the statistical significance  
1019 between two treatments.

1020 **Fig. 8** Thermal performance curves based on specific growth rates ( $d^{-1}$ ) of *Emiliana*  
1021 *huxleyi*, including our experimentally determined constant **condition temperature**  
1022 **performance curve** (black symbols and solid line) and a predicted fluctuating  
1023 **condition temperature performance curve** (dashed line) according to the model of  
1024 Bernhardt et al. (2018). Measured growth rates from the two low and high  
1025 temperature experiments are shown for constant thermal conditions (red symbols),  
1026 one-day (green symbols) and two-day (blue symbols) variation treatments.

1027

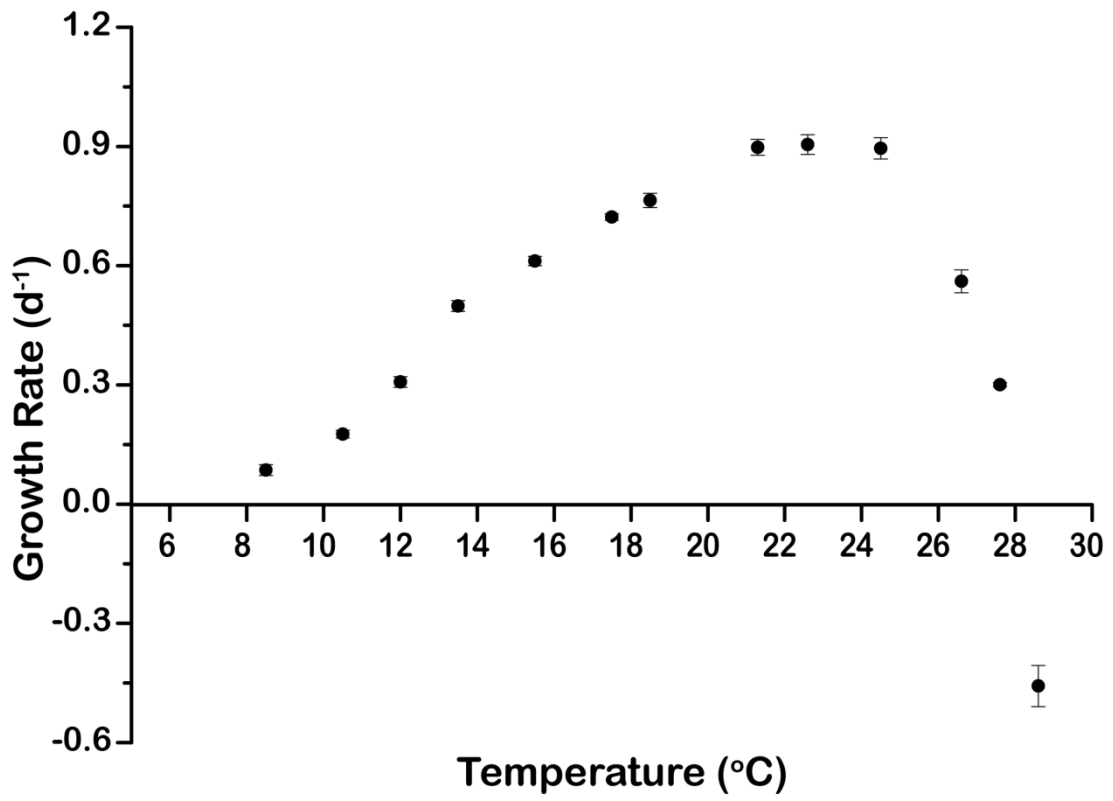
1028 **Table 1** The effect of temperature variation under low and high temperature on total carbon (pg/cell), cellular POC (pg/cell), cellular PIC (pg/cell), cellular PON  
 1029 (pg/cell), cellular POP (pg/cell) and cellular Chl *a* (pg/cell) of *Emiliana huxleyi*.

| Treatment               |                         | Total Carbon | Cellular PON | Cellular POP | Cellular POC | Cellular PIC | Cellar Chl <i>a</i> |
|-------------------------|-------------------------|--------------|--------------|--------------|--------------|--------------|---------------------|
| <b>Low temperature</b>  | 18.5 °C                 | 11.5±0.4     | 1.8±0.2      | 0.17±0.00    | 8.0±0.6      | 3.5±0.3      | 0.14±0.00           |
|                         | One-day cool point (16) | 13.0±0.5     | 2.2±0.3      | 0.18±0.00    | 8.9±0.3      | 4.1±0.3      | 0.15±0.01           |
|                         | One-day warm point (21) | 12.0±0.7     | 2.1±0.3      | 0.19±0.00    | 9.3±0.9      | 2.7±0.9      | 0.19±0.00           |
|                         | Two-day cool point (16) | 10.1±0.7     | 1.3±0.2      | 0.16±0.01    | 6.0±0.9      | 4.0±0.3      | 0.12±0.01           |
|                         | Two-day warm point (21) | 10.4±0.5     | 1.5±0.2      | 0.17±0.01    | 6.6±0.5      | 3.8±0.3      | 0.15±0.01           |
| <b>High temperature</b> | 25.5 °C                 | 15.0±0.7     | 2.0±0.1      | 0.21±0.01    | 9.5±0.3      | 5.5±0.7      | 0.18±0.02           |
|                         | One-day cool point (23) | 16.1±1.4     | 3.0±0.2      | 0.21±0.00    | 12.9±1.5     | 3.2±0.2      | 0.15±0.01           |
|                         | One-day warm point (28) | 19.1±0.8     | 4.4±0.3      | 0.24±0.01    | 17.0±0.6     | 2.1±0.2      | 0.20±0.02           |
|                         | Two-day cool point (23) | 12.4±1.0     | 1.9±0.2      | 0.19±0.01    | 7.5±1.0      | 4.8±0.3      | 0.13±0.01           |
|                         | Two-day warm point (28) | 19.4±2.0     | 3.9±0.8      | 0.25±0.03    | 18.3±3.7     | 2.1±0.9      | 0.25±0.02           |

1030

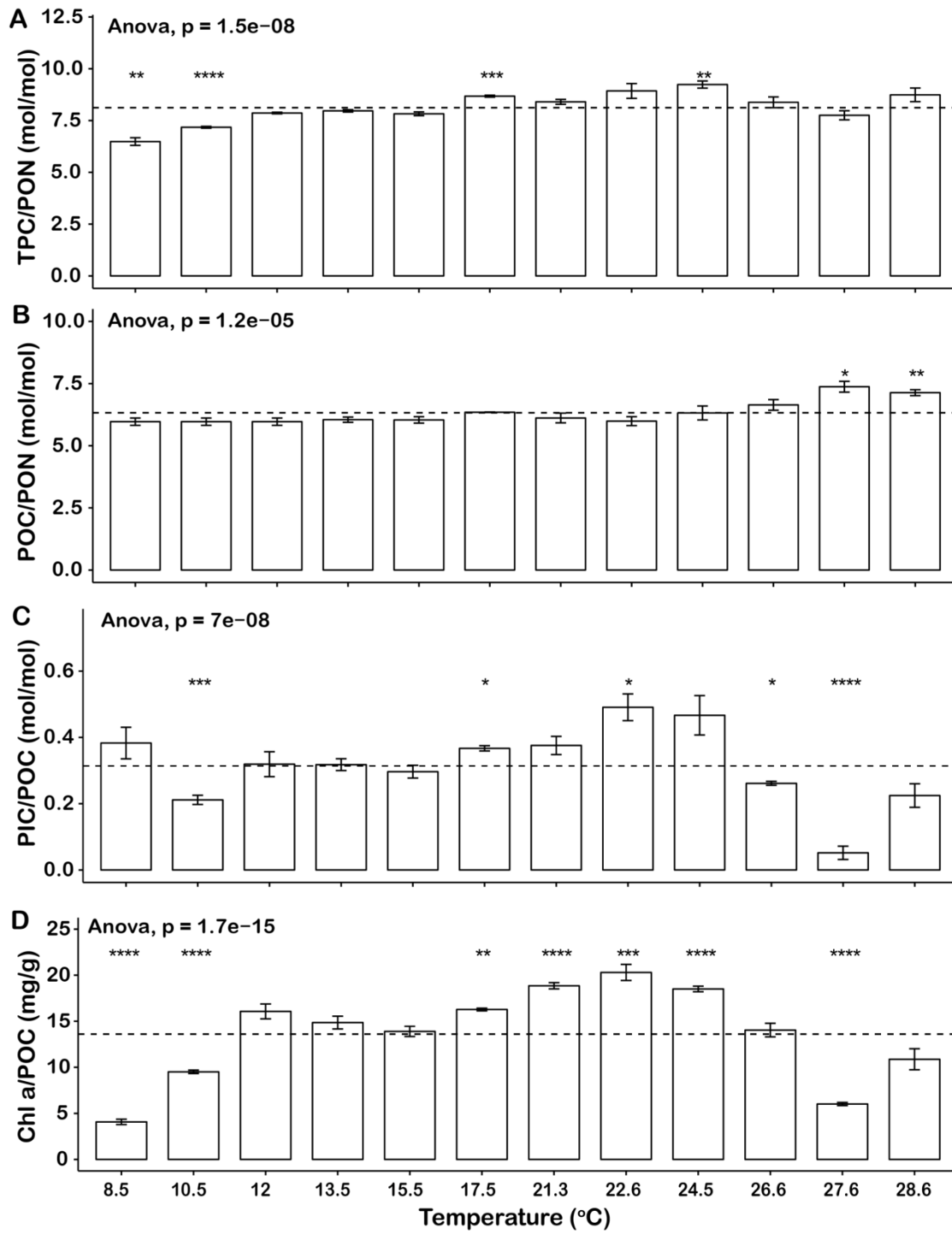
1031

1032 Fig. 1



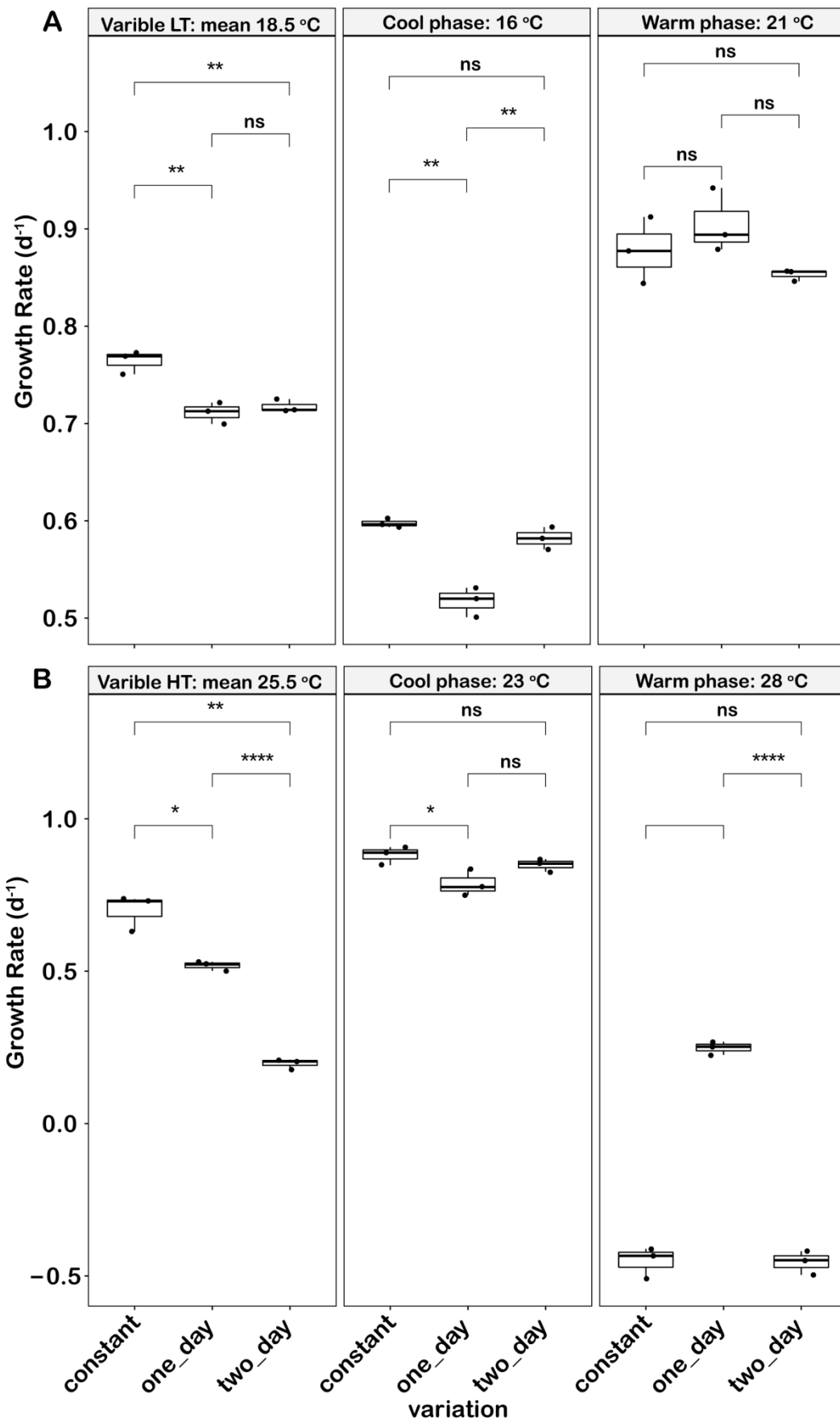
1033

1034 **Fig. 2**

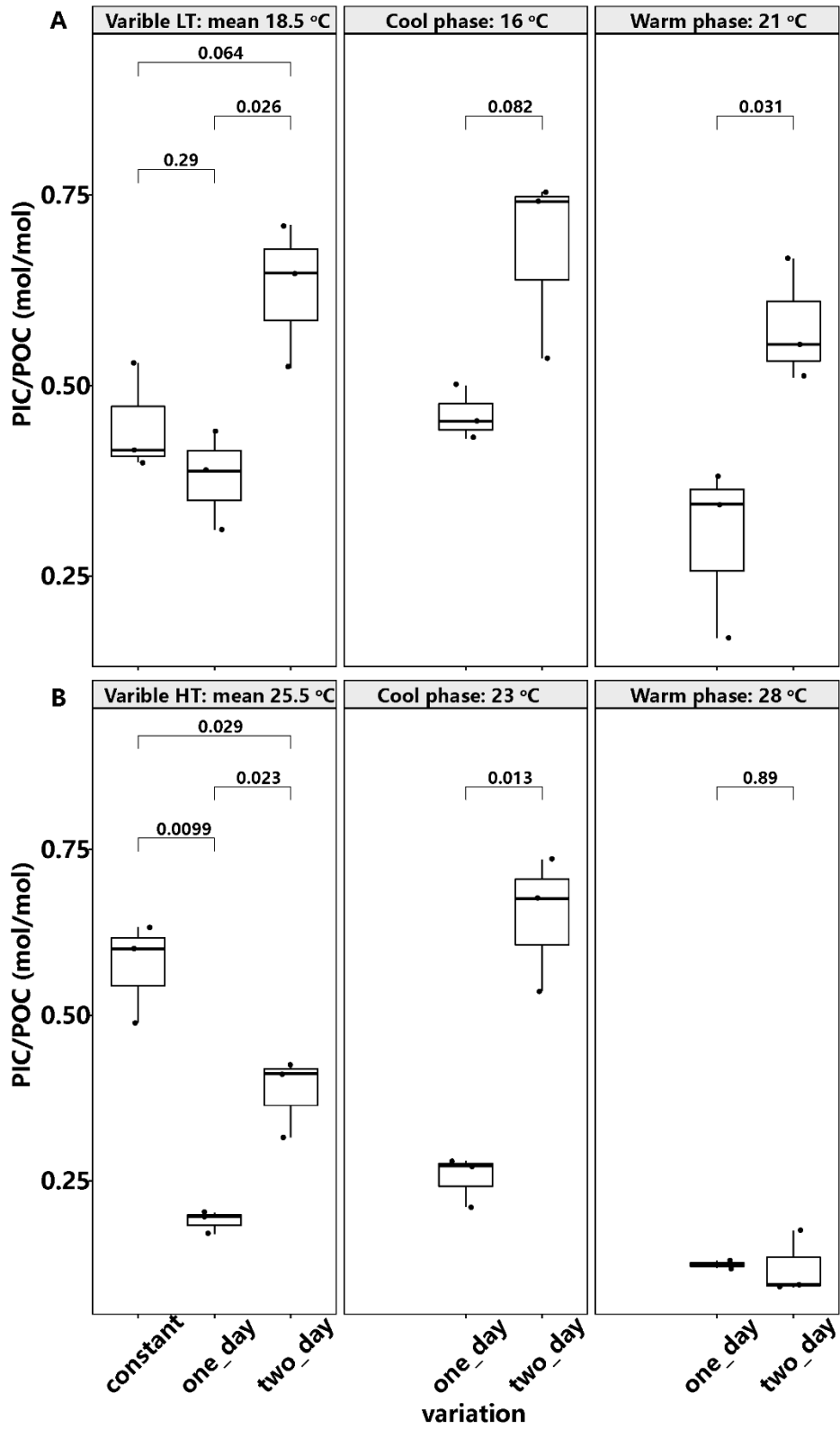


1035

1036



1039 **Fig. 4**

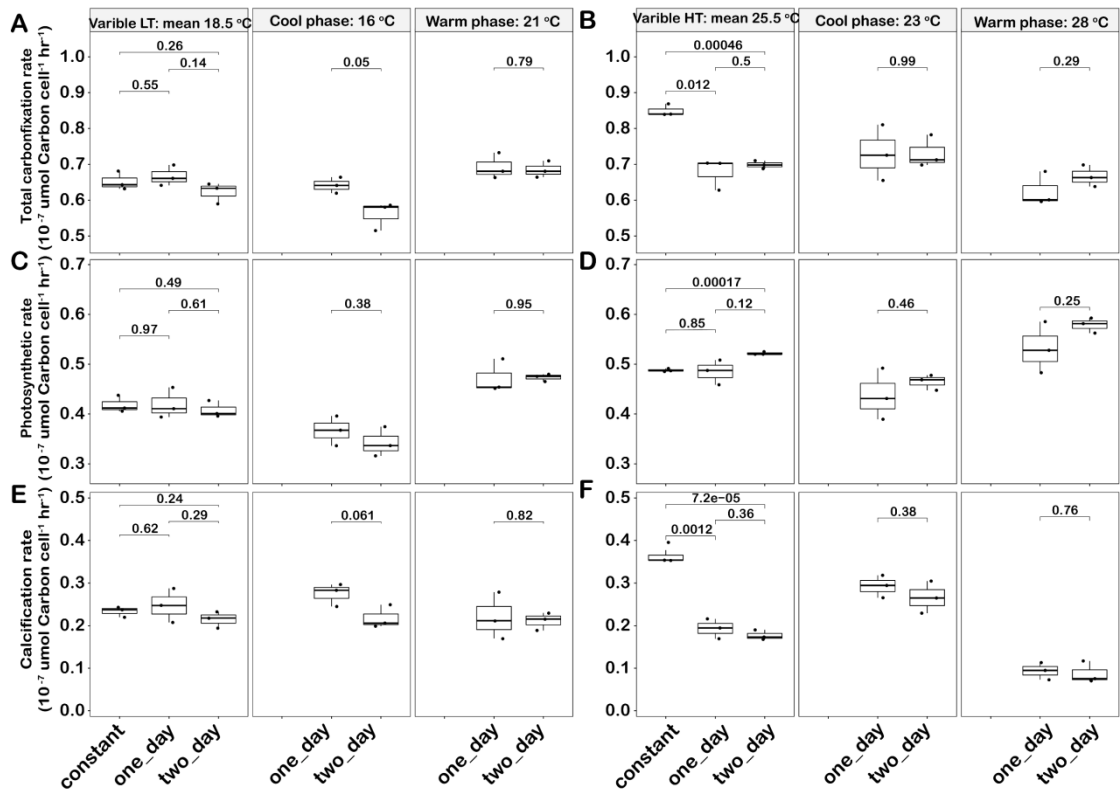


1040

1041

1042 **Fig. 5**

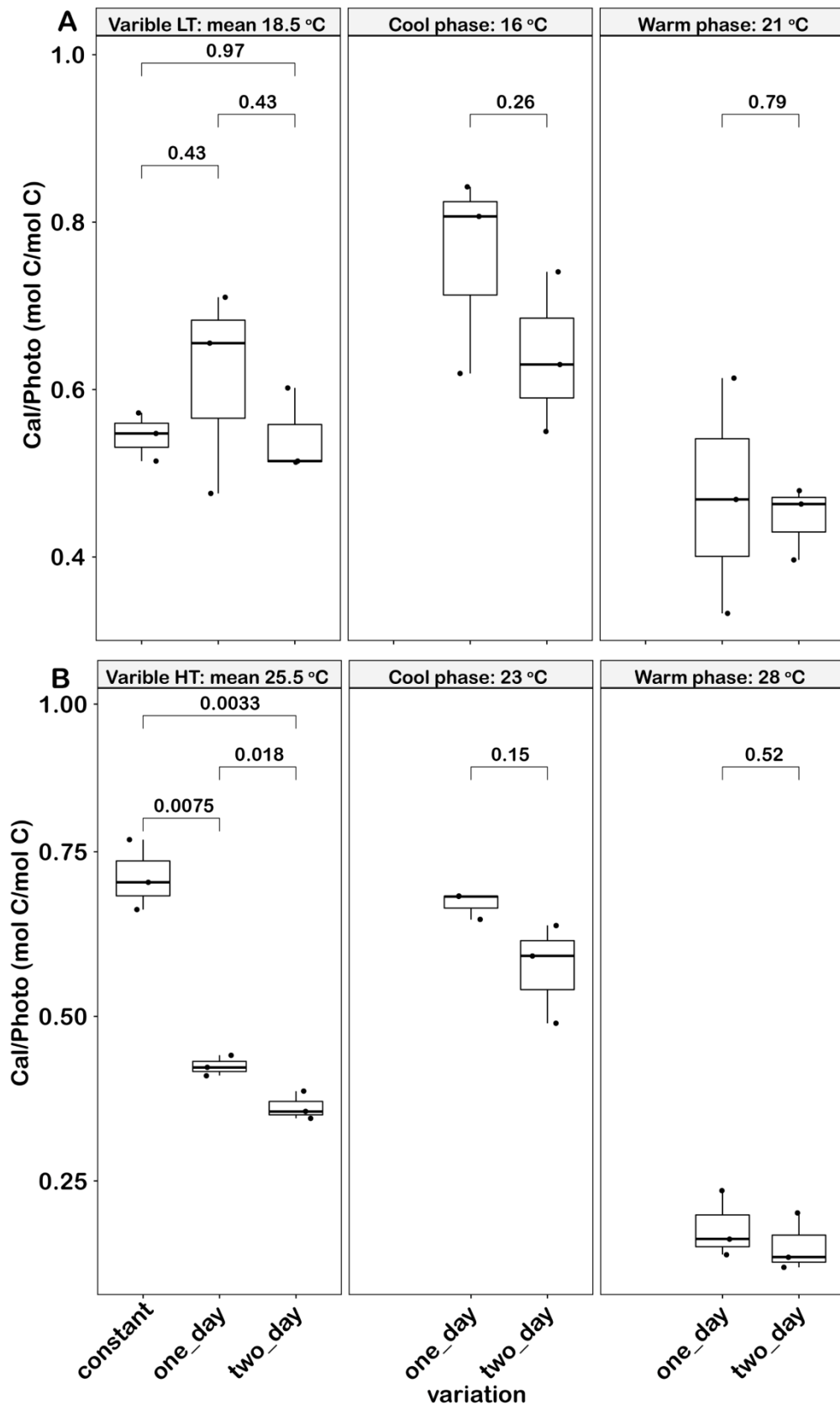
1043



1044

1045

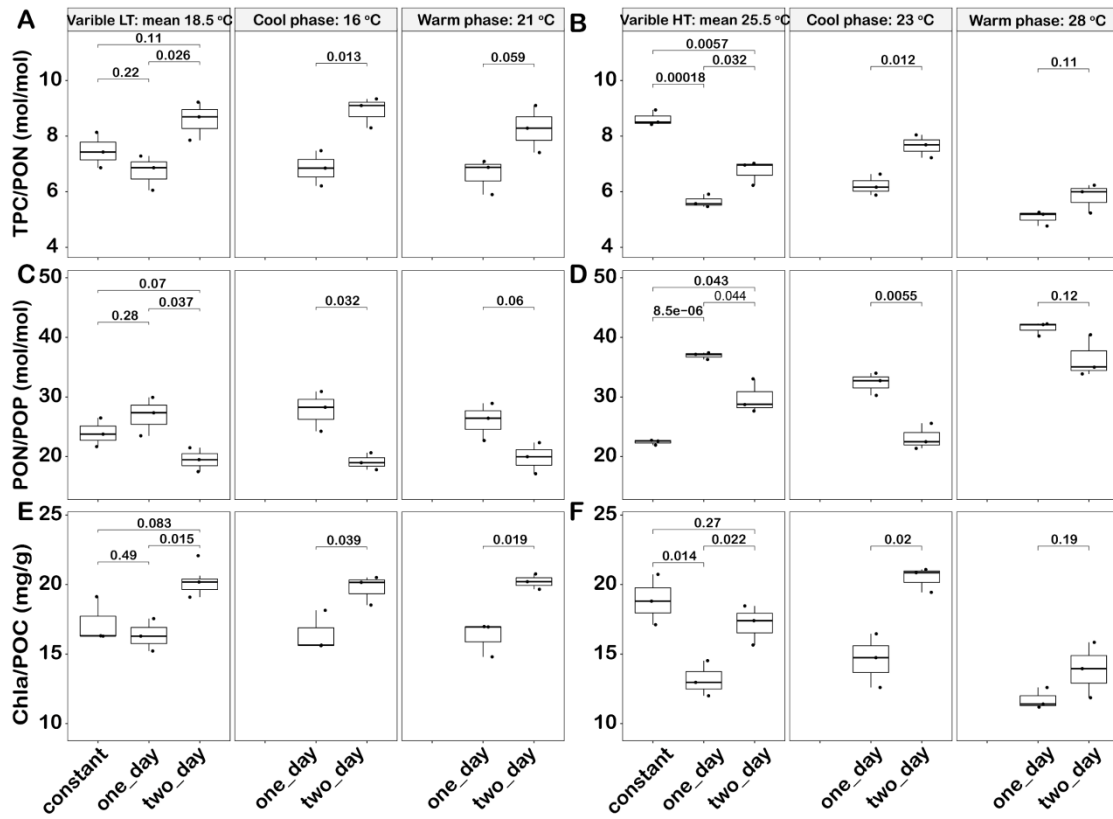
1046 **Fig. 6**



1047

1048

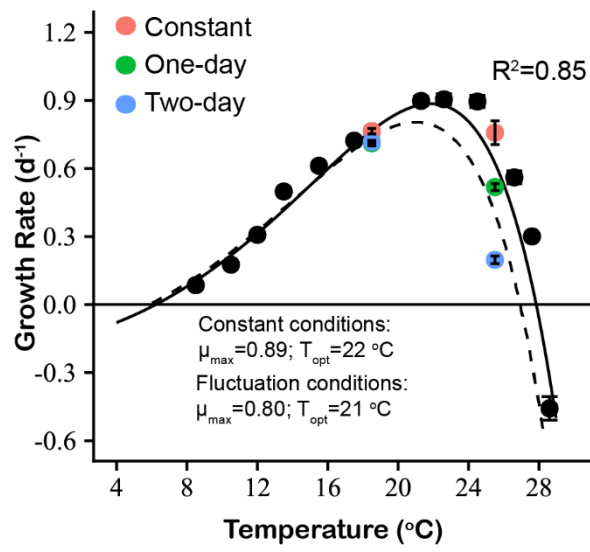
1049 **Fig. 7**



1050

1051

1052 **Fig. 8**



1053